NTNU – Trondheim
Norwegian University of
Science and Technology

SAND & FINES IN MULTIPHASE OIL AND GAS PRODUCTION

Udoh Richard Richard

SAND AND FINES IN MULTIPHASE OIL AND GAS PRODUCTION

Richard, Richard Udoh

Trondheim

July 2013

ACKNOWLEDGEMENT

This thesis work, TPG 4920 was carried out in partial fulfillment of the requirements for my Masters' degree in Petroleum Production Engineering in Norwegian University of Science and Technology, NTNU.

I would like to thank my supervisor, Professor Jon Steinar Gudmundsson for his efforts and time taken to go through my work thoroughly and giving invaluable advices and assistances where necessary.

I want to appreciate all those involved and responsible for the success of this Masters' programme, Dr. Uduak Mme, Rita Kumar, Professor Pal Skalle, Tone Sanne and a host of others. A big thanks to Tolu Adeosun, Tosin Ajayi, my family, friends and well-wishers, who were always there to give me the much needed support.

I would finally like to gratefully thank my creator, the Almighty God for His grace and mercies, which has been sufficient to see me through this programme.

ABSTRACT

This thesis work focuses on multiphase flow in the oil and gas industry. As differences in temperatures and pressures come to play from the reservoir to the surface, in tubing and in pipelines, gas tend to dissolve and evolve out from oil, with water and solid particles making their way into the production flow stream, giving rise to a multiphase gas-liquid-solid production and transportation. A review of sand and fines production worldwide was carried out and concluded that sand production is a common occurrence in the petroleum industry, present in all the major oil producing regions of the world. Multiphase flow patterns were equally discussed in this work stating the different flow regimes available in the vertical and horizontal pipe system. HYSYS was used to obtain fluid properties for volatile oil used in the determination of major parameters such as fluid velocities, hold-ups and pressure drop. Results did show that particle velocity to a large extent depended on the fluid velocity, which would always be higher with increasing amounts of gaseous phase present as experienced in annular and slug flow. The velocity profile chart showed the sand peak velocities in annular and slug flow as 13.2 m/s and 9.8 m/s. It was also observed that pressure drop along a pipe will under normal conditions tend give a positive slope when plotted against superficial fluid velocities.

TABLE OF CONTENTS

LIST OF TABLES

LIST OF FIGURES

NOMENCLATURE

A (m^2)   Cross-sectional area of pipe

C_D (-)   Drag coefficient

D (m)   Pipe diameter

d_P (m)   Solid particle diameter

d_{50} (m)   Cut size

E (-)   Entrainment fraction

f (-)   Friction factor

F_B (N)   Buoyancy force

F_D (N)   Frictional drag force

F_G (N)   Gravitational force

F_M (N)   Momentum transferred force

F_P (N)   Particle interaction force

F_V (N)   Viscous force

g (m/s^2)   Gravitational acceleration

H_F (-)   Liquid hold-up fraction in
                                   liquid film

H_L (-)   Liquid hold-up

H_{LS} (-)   Liquid hold-up fraction in slug
                                   body

H_O (-)   Overall hold-up

H_S (-)   Sand hold-up

L_F (m)   Length of liquid film

L_{LS} (m)	Length of liquid slug body
m_s (Kg/s)	Input solid mass rate
m_P (Kg)	Mass of particle
N_{Fr} (-)	Froude Number
Δp_f (Pa/m)	Frictional pressure drop
Δp_{o-w} (Pa/m)	Pressure drop of oil-water flow
Δp_{o-w-g} (Pa/m)	Pressure drop of oil-water-gas mixture
R (m)	Pipe radius
Re_P (-)	Particle Reynolds number
u_∞ (m/s)	Terminal settling velocity
v_e (m/s)	Erosional velocity
v_F (m/s)	Velocity of liquid film
v_G (m/s)	Gas velocity
v_M (m/s)	Mixture velocity
v_O (m/s)	Bubble rise velocity
v_{LS} (m/s)	Velocity of slug body
v_P (m/s)	Particle velocity
v_r (m/s)	Radial liquid velocity
v_S (m/s)	Sand velocity
v_{SG} (m/s)	Superficial gas velocity
v_{SL} (m/s)	Superficial liquid velocity
v_{SS} (m/s)	Superficial solid (sand) velocity
v_t (m/s)	Minimum transport velocity
x (-)	Local weight fraction of gas

δ (m)	Liquid film thickness
ρ_G (Kg/m^3)	Gas density
ρ_L (Kg/m^3)	Liquid density
ρ_M (Kg/m^3)	Mixture density
ρ_P (Kg/m^3)	Particle density
μ_f (Pa.s)	Fluid viscosity
ω (m/s)	Angular velocity

CHAPTER 1
INTRODUCTION

Multiphase flow is evident in many different areas of science and engineering, these include: sediment transport in river streams, transport of colloids in rain-water, slurry pipeline transportation, drill cuttings removal and transport of fracture proppants (Doan, et al. 1993). It is the most commonly experienced kind of flow in the petroleum industry, and could occur as two-phase, three-phase and/or four-phase flow, which could be as a result of the inclusion of sand and fines to a gas-oil-water multiphase flow.

Sandstone reservoir happens to be the source for most of the worlds' hydrocarbons. Approximately 70% of oil and gas reservoirs worldwide are unconsolidated. (Chen, et al. 2010). This implies that a good number of oil and gas fields are challenged with sand and fines production issues worldwide. The production of formation sand along with reservoir fluids is one of the oldest problems faced by oil companies and has proven to be one of the toughest to solve. (Maryam 2010).

Schlumberger (2013) defined sand production as the migration of formation sand caused by the flow of reservoir fluids. It begins when the rock around the perforations fails, and the fluids can push the loose grains into the wellbore. (Eriksen, et al. 2001). Sand production is a process that develop progressively in three stages: failure of rocks surrounding an open hole or perforation from which free sand grains are generated, disaggregation of sand

particles from failed material, and transport of those free grains by the effluents into the wellbore and up to the surface (Sunday and Andrew 2010). It is clear that sand particles have to be disintegrated from its parent rock first, before it can flow along with the reservoir fluids in the wellbore. This happens when the reservoir rock has low formation strength and fails under the in situ stress conditions and the imposed stress changes due to the hydrocarbon production. (Maryam 2010).

Taking a closer look into the fluid dynamics, two major types of interactions is said to occur in a multiphase flow. Doan, et al. 1993 states them as:

Interphase interaction, where the fluid phase interacts with the particulate phase. Drag force is exerted on the particles by the fluid stream and momentum is transferred from one phase to another, and *Intraphase interaction,* where solid particles in the particulate phase interact with each other. It is characterized mainly by the frequency of particle-particle collision.

It is no longer news that severe operational problems could result from the production of formation sand. These problems range from erosion and damage of downhole and surface equipment such as valves, pipelines, separators etc. to inhibition of production through well clogging. These issues could be mild or severe depending on the flow rate and viscosity of the produced fluid, and the rate of production and accumulation of fines and sand grains. Sand production costs oil companies tens of billions of dollars yearly (Wu and Tan 2005).

This work is a continuation of previous project work on sand transport by oil in tubing and pipelines. The main objectives of this masters' thesis work is to discuss multiphase production of hydrocarbons in the presence of solid particles, present methods that are used to predict the production of sand and fines from reservoir formations, transport of sand and fines (in multiphase flow of oil, gas and water) from bottom hole to well head, and in pipelines.

CHAPTER 2
LITERATURE REVIEW

2.1 Review of Sand & Fines Production Worldwide

The production of sand as will be shown in this chapter is a worldwide issue, experienced in the North Sea, Gulf of Mexico, Middle East and Gulf of Guinea, where most of the world's hydrocarbon is sourced.

2.1.1 Gullfaks and Statfjord, Norway

Based on a study carried out by Andrews et al. (2005), on sand management on Statfjord and Gullfaks fields. It was discovered that, oil production on Statfjord, was 22000 Sm3/d at the end of 2004, with an average water cut of 85% and GOR of 720 Sm3/Sm3. Oil production on Gullfaks was 30000 Sm3/d with an average water cut of 75% and GOR of 200 Sm3/Sm3.

The sand production on each platform is estimated to be 50 to 100 tonnes/yr. Individual well sand production can be up to 5 tonnes/yr. Two-thirds of the ±90 active production wells on each field, are presently limited by sand production. The mean grain size for the different formations is 200 microns while the d_{50} size ranges from 100 to 700 microns. Gullfaks reservoir formation is unconsolidated and perforated completions will produce sand regardless of perforation design and well inclination.

The cumulative probability plot of total sand production on Statfjord, is shown in Figure 1. The concept of sand management in these fields is based on control and monitoring of well rates, sand influx and erosion. Produced sands, which settle in the separators, are flushed through jetting of the separators with seawater. This action is carried out from time to time without any production constraints. The jet water from the first, second and test separators is directed to the produced water flash drum.
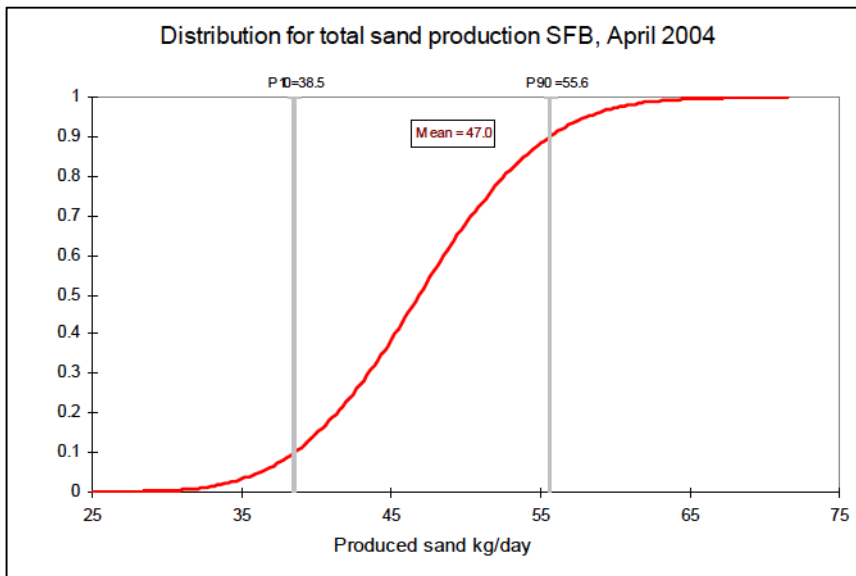
Figure 1: Distribution for total sand production during normal day on Statfjord (Andrews et al. 2005)

2.1.2 Varg, Norway

According to a paper by (Eriksen, et al. 2001), the Varg field is located in the Norwegian sector of the North Sea. It consists of a not-normally-manned wellhead platform (WHP) with dry wellheads and floating production storage offloading (FPSO) vessel for processing the crude. The reservoir is heterogeneous sandstone of upper Jurassic age, with estimated reserves of approximately 35 million STB. The fields cover an area of 7 km2, and the depth to the top of the reservoir is at 2720 m below sea level.

Sand production was experienced during the drillstem testing performed in some of the appraisal wells.

Table 1 shows sand production over several hours. In this field, sanding issues were addressed at an early stage, which gave the opportunity to review different options of sand management and selection of cost effective means of sand control.

Table 1: Well A-sequence of events with respect to sand production (Eriksen, et al. 2001)

Hour	Choke	Event
15.29		Well Perforated
16.28	48/64	Sand plugging the choke- BS &W line plugged
16.55	36/64	BS & W 7% sand
17.00	32/64	Plugging problems
17.17	36/64	BS & W 1% sand
17.33	36/64	BS & W traces of sand
17.47	36/64	BS & W 0% sand- divert to 48/64 choke
17.48	48/64	Plugging- increased to 64/64 choke
17.55	64/64	Traces of sand
18.05	52/64	Got a peak on sand detector, indicating more sand
		lifted out of the string owing to increased rate
22.06	32/64	Cease of flow owing to choke plugging

2.1.3 Northwestern Canada

Yarlong and Carl (2001) wrote a paper on enhanced oil production due to sand flow. The area of interest was northwestern Canada (heavy-oil reservoirs) and North Sea (conventional oil reservoir). Field data for solid production and enhanced oil production, collected from about 40 wells in the Frog Lake area (Lloydminster, Canada), are used to validate the model for the cumulative sand and oil production.

Numerical results indicate that sand production could reach up to 40% of total fluid production at the early production period and drop down to a minimum level after the peak. Results from

Lindbergh and Frog Lake in Lloydminster fields, indicate that primary recovery is dependent mainly on the processes of sand production and foamy-oil flow.

Optimization of oil production, keeping sand production under control is the challenge being faced in these fields. However, reduced oil flow or zero production often results with sand control, especially in heavy-oil reservoirs. For example, it has been observed that an average oil production of only 0.0 to 1.5 m^3/d can be achieved in a well with no sand production allowed, while 7 to 15 m^3/d oil may be produced with sand production. It can be seen that sand production corresponds to increase in oil production in these reservoirs, which could be either as a result of a higher reservoir mobility or development of highly permeable zones due to sanding.

This is a case where sand production has its good and bad sides, because encouraging sand production enhances oil production, on the other hand, leads to increase in oil production cost due to sanding and environmental problems. Hence, a quantified model linking sand rate and reservoir enhancement to forecast the economic outcome of sand production was developed.

Figure 2 shows the average sand production performance in Frog Lake and Lindbergh reservoirs, using the proposed model. The average cumulative sand production curve is based on data for sand production from approximately 40 wells.
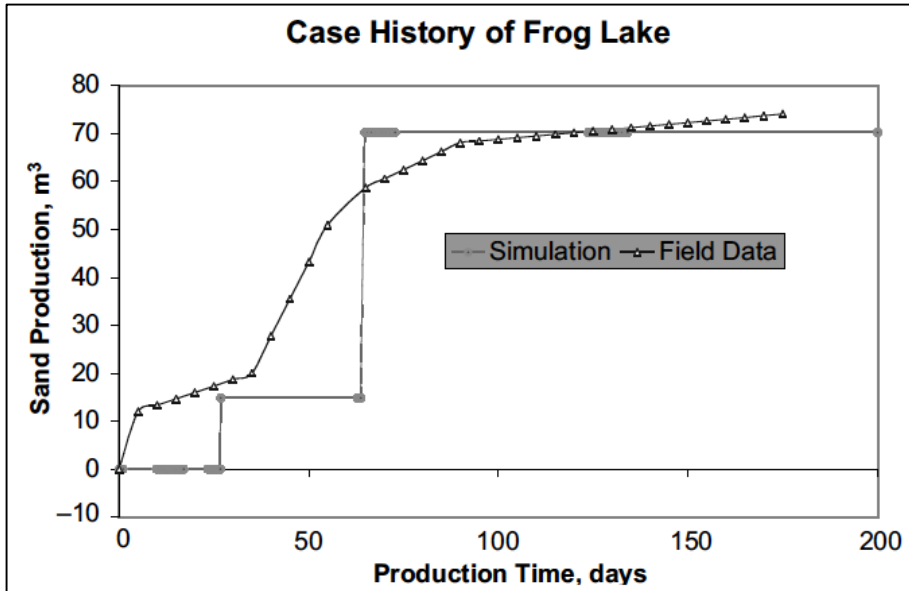
Figure 2: Simulated sand production versus Field data from Northwestern Canada (Yarlong and Carl 2001)

2.1.4 Zulia, Venezuela

According to a paper by Hong'en et al. (2005), Intercampo oilfield located in Zulia of western Venezuela is an unconsolidated sand reservoir, characterized by heavy crude and mid-high permeability. Most of these reservoirs are buried from 3560 feet to 7500 feet and heavy crude oil gravity ranges from 12.5-23.3 API. In recent years, horizontal well technology has been used extensively in the production of heavy oil. The major challenge in this unconsolidated reservoir is dealing with the sand production that comes along with the heavy crude oil production into the horizontal well. It is therefore of utmost

9

importance to predict sand production and optimization completion method. Table 2 shows a sand production prediction using one of the most accurate prediction methods, combination modulus, E_C. E_C is measured in $10^6 psi$ and $E_S \times E_B$ is measured in $10^9 psi$. E_C and $E_S \times E_B$ are discussed later in chapter 4 (Page 48)

Table 2: Prediction comparison combination modulus with acoustic time modulus (Hong'en et al. 2005)

Well No.	Parameter	Poisson Ratio	Max.	Min.	Mean	Sand Production
BA744	E_C	-	1.868	0.81	1.14	Worse
		0.2	4.599	0.865	1.75	Possibility
	$E_S \times E_B$	0.3	4.338	0.816	1.62	Possibility
BA2295	E_C	-	2.907	0.291	0.01	Possibility
		0.2	11.145	0.112	1.66	Free or possibility
	$E_S \times E_B$	0.3	10.513	0.105	1.57	Free or possibility
BA2297	E_C	-	1.68	0.855	1.11	Worse
		0.2	9.63	3.72	1.66	Possibility
	$E_S \times E_B$	0.3	3.51	0.908	1.57	Possibility
BA2313	E_C	-	1.519	0.711	1.07	Worse
		0.2	2.868	0.628	1.44	Possibility
	$E_S \times E_B$	0.3	3.003	0.658	1.51	Possibility
BA2326	E_C	-	1.824	0.804	1.16	Worse
		0.2	4.388	0.853	1.82	Possibility
	$E_S \times E_B$	0.3	4.139	0.805	1.72	Possibility

2.1.5 Saudi Arabia

Abass, et al. (2002) analyzed five sandstone reservoirs in Saudi Arabia and two of them indicated sand production, as seen in Figure 3.
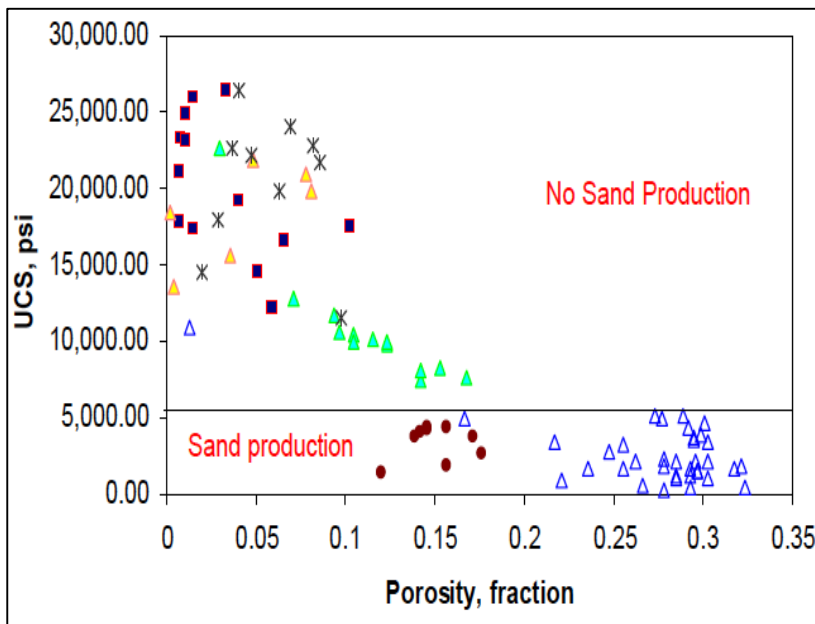
Figure 3: Characterization of sanding tendencies based on UCS-Porosity correlation on 5 reservoirs in Saudi Arabia (Abass et al. 2002)

Uniaxial compressive strength (UCS) as defined by encyclopedia 2013, simply refers to the strength of a reservoir rock when a compressive force is applied in one direction without lateral constraint. The two reservoirs with sanding tendencies (Figure 3) have UCS less than 6000 psi and porosity greater than 13%.

As earlier mentioned in this work, flow rate amongst other factors could affect sand production. Abbas et al. (2002) further goes to show this in Figure 4, using a field in Saudi Arabia (Safaniya field) as a case study.
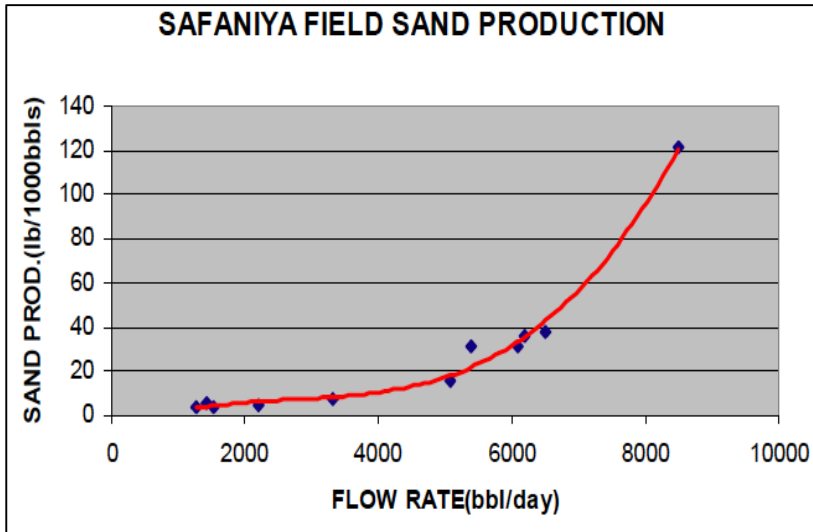
Figure 4: Field correlation between production rate and amount of sand produced (Abass et al. 2002)

There is a critical production rate below which sand production is manageably decreased, though this rate could be at an uneconomical production level. It is therefore worthwhile to ascertain this critical production rate before completion strategy design for a given formation. (Abass et al. 2002)

2.1.6 Iran

Reza et al. (2010) carried out studies in the Persian oil fields, based on successful application of expandable sand screen. From his report, it is seen that more than 80% of Iran oil reservoirs are carbonate and about 20% are sandstone. Asmari formation is where the main sandstone reservoir layers are. The Asmari oil fields of Iran are huge, most of them having recoverable reserves greater than 1 billion bbl each and many having much more. There have been reports of sand production problems at Asmari reservoir since 1940. The unconsolidated sandstone layers are the main reason of sand production in this reservoir. Expandable sand screen (ESS) was recently installed as a sand control method. The outcome was successful, as shown in Figure 5. A comparison was performed in oil production before and after installation of ESS during one year.
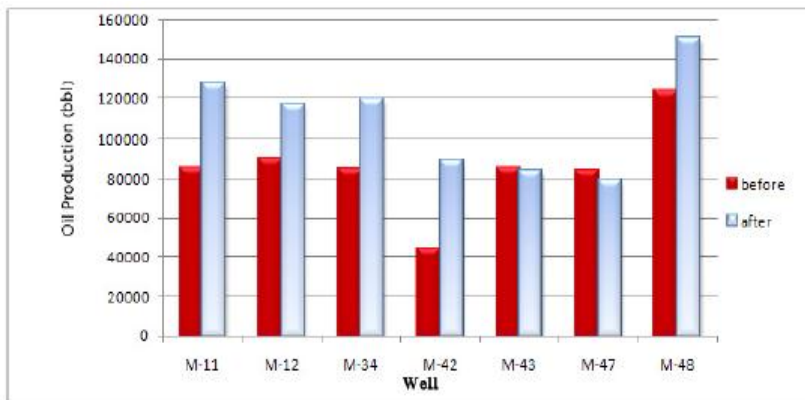
Figure 5: Average oil production of each well in one of the fields before and after ESS installation (Reza et al. 2010)

It can be said that ESS technique is a good alternative for Iranian sandstone reservoirs, based on the outcome of oil production in the Persian fields after a year.

2.1.7 Bongkot Field, Gulf of Thailand

Based on a study by McPhee et al. (2000), sand production is also an issue in Bongkot field, Gulf of Thailand as it has led to significant incremental costs and increased the risk of potential key flowline and failures of control equipment. PTT Exploration and Production (PTT-EP) is in charge of operations in the Bongkot field in Gulf of Thailand. Production started in July 1993, minor sand production was observed in few wells by 1994 and by November 1999, sand production was reported from 18 wells. Over 300 tonnes of sand were removed from separators and water treatment facilities in 1999.

2.1.8 Beibu Gulf of South China Sea

Pingshuang et al. (2000) carried out a research on south of China Sea on sand production prediction. It was discovered that most of the China offshore oilfields are on unconsolidated sand reservoir and different levels of sand production is experienced across these fields. The reservoir rocks in Beibu Gulf of South China sea are situated between unconsolidated and consolidated. Some sands were seen in the surface oil/gas separator during drillstem test (DST) operation for two particular wells in this region. The sand was observed to occupy half the volume of the separator.

2.1.9 Niger-Delta, Nigeria

Sand production is currently one of the major challenges being faced by the petroleum industry in the Niger-Delta, as millions of dollars are lost every other year due to restricted production rates, well cleaning and work over operations. (Adeyanju and Oyekunle, 2011).

Vincent et al. (2012) did carry out some analysis in the Niger-Delta region of Nigeria. The following review is based on their analysis. As at late 2012, the total amount of discovered recoverable oil and gas in the Niger-Delta were put at 34.5 billion barrels and 93.8 trillion cubic feet respectively. This makes the Niger-Delta one of the biggest hydrocarbon provinces worldwide, and is ranked twelfth largest in the world. The Niger-Delta is divided into five depo-belts, separated by major syn-sedimantary faults zones. They are: Central Swamp, Coastal Swamp, Greater Ughelli, Northern Delta and Offshore depo-belts. These depo-belts make up the most active part of the delta in terms of structure and deposition.

In Nigeria, oil accumulations are generally of small areal extent, usually faulted and characterized by thin oil columns often with overlying gas caps. These accumulations occur in Miocene sands, such that only loosely consolidated formation is seen to a depth of 10000 feet. As a result, sand control is not installed at depths greater than 10000 feet, but rather at shallower completions. The porosity of the formation ranges from 25 to

35%, with mostly fine grained and well-sorted sand; permeabilities range from 0.5 to 5 darcies.

2127 wells were analyzed across the 5 depo-belts in the Niger-Delta. It was discovered at the end of the analysis that 64% of the wells analyzed were sand producers and that the coastal swamp is the most drilled region in the Niger-Delta, while the Greater Ughelli stands out as the most prolific sand producing region in the Niger-Delta with over 90% of its reservoirs producing sand, irrespective of sand control and formation depth. This is shown in Figure 6. Conduit is used in place of wells in the figure below, thus conduit count refers to the number of wells.
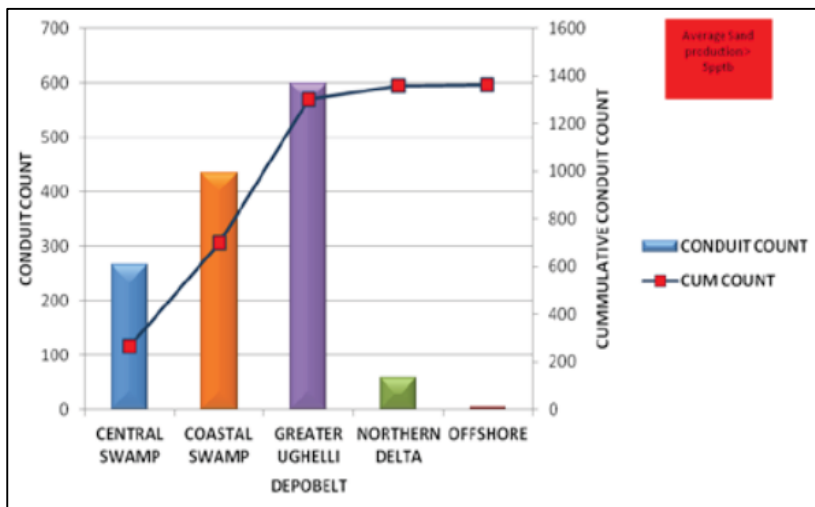
Figure 6: Sand producing wells according to depo-belts in the Niger-Delta (Vincent, et al. 2012)

After a study conducted by Sunday and Andrew (2010), on selected oil fields in the Niger-Delta, it was discovered that Gas-Oil ratio (GOR) and water-cut contributed to sand production either individually or as a combination. Other reason for sand production in the Niger-Delta has to do with its weakly consolidated or unconsolidated formation (Abubakar, et al. 2012).

2.2 Effects of Water Cut on Sand and Fines Production

Water production increase towards the late life of an oil and gas field is inevitable. This may be due to water coning or water injection. On the average nowadays, oil companies produce three barrels of water per barrel of oil. (Wu and Tan 2005). On most occasions in the field, the initiation of sand production has been observed to coincide with water breakthrough. Thus, it is generally believed that water production increases the risk of sand production in a field. The effect of water cut on sand production is of major importance to the petroleum industry. (Wu and Tan 2005). These effects as described by Wu and Tan (2005), include:

- Reduced capillary bond between originally water-wet sand grains;
- Chemical interaction between rock matrix and water as a result of increased water saturation; and

- Relative permeability effect resulting in increase in drag force for mobilizing sand grains from failed parent materials.

Increase in water saturation has a strength reducing effect on all types of rock. This effect varies depending on the kind of rock. An illustration of this is shown in Figure 7.
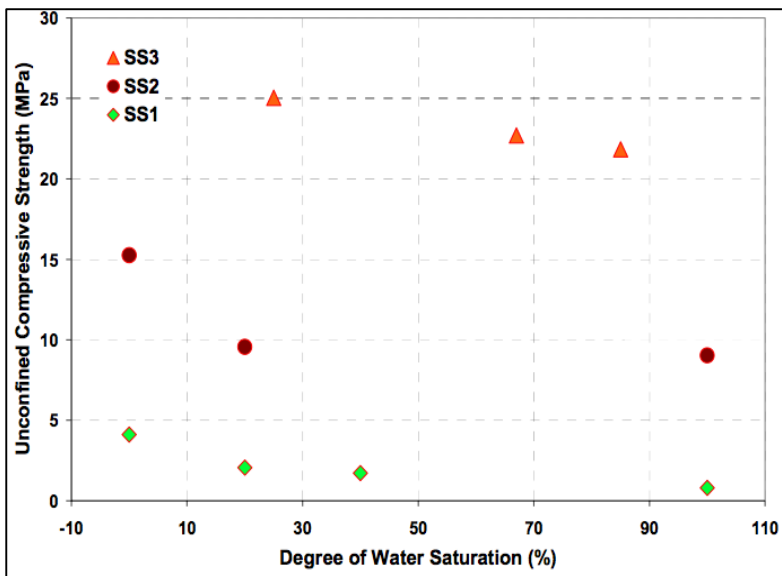
Figure 7: Effect of water saturation on rock strength for three sandstones: SS1, SS2 and SS3 (Wu and Tan 2005)

It can be observed from Figure 7 above that, the main reduction in rock strength was between 0% (dry rock) to 20% water saturation. Wu and Tan (2005) did observe from their study that the further reduction in rock strength depended on the clay content of the rock material. It was deduced that the effect of

water cut is to reduce rock/perforation strength, thereby encouraging sand production and this effect depends on the mineralogical content of the rock, i.e. the effect is more significant for sandstones with high clay content and low residual water saturation.

Luo et al. 2012 carried out some tests and analysis using cores and crude oil from an unconsolidated reservoir in Eastern China, block Z43. It was observed as water saturation increased from 20% to 80% due to water injection, it led to permeability decrease by 80% as a result of its high clay content and a significant increase in sand production.
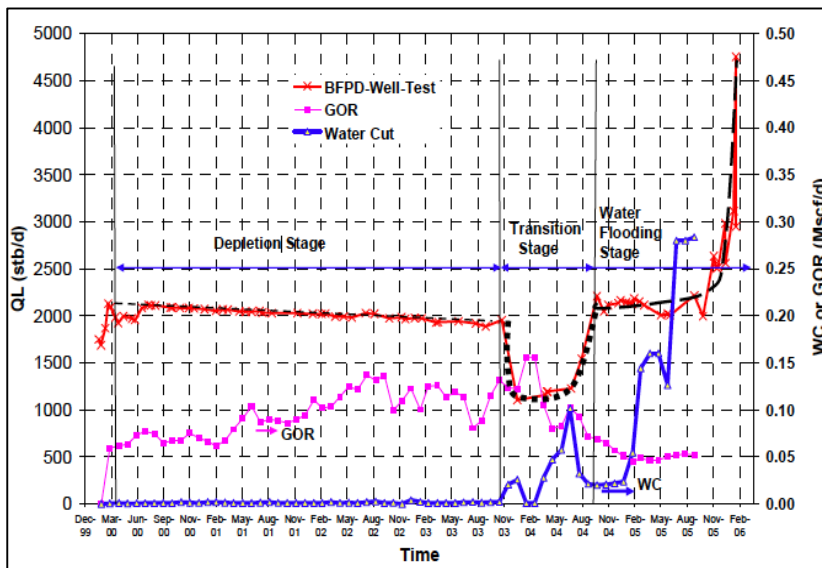
Figure 8: WC, GOR and QL history for a well in Angola (Tang, et al. 2007)

Figure 8 shows the production history of an oil well in Angola divided into three stages:

- Depletion Stage (2000 to 2003): No water production and GOR increased during this stage.
- Transition Stage: (2003 to 2004): the well started producing little amounts of water and GOR started declining.
- Water Flooding Stage (2004 to 2006): water cut rose clearly and GOR declined below original levels.

(Tang, et al. 2007)

It is safe to infer from all these, that in the lifetime of an oil and gas well, the greatest risk for sand production is experienced in the late life of the field when the reservoir pressure depletes or water breaks through.

2.3 Wellbores and Pipelines

Oil and gas wells have conventionally been drilled vertically. This has been the trend for many decades until technological advances came up with other methods to drill that now allow deviation from the straight line drilling. Thus wellbores and pipelines vary in shapes in line with the drilling method applied. The major types are the vertical and horizontal wells/pipes.

2.3.1 Vertical wellbore/drilling

This is the traditional type of drilling, where the wellbore is drilled straight down until the pay zone is reached. This type of

drilling is most efficient when the formation has high permeability and reservoir pressure. However, vertical drilling is not always the most economic approach taking into consideration restricted surface access, reservoir pressure and geology. (Cathedral Energy 2013)

2.3.2 Horizontal and Slant wellbore/drilling

Horizontal drilling involves drilling a well from the surface to the subsurface just above the pay zone called a kickoff point, then deviating the wellbore from the vertical to make a curve which intersects the reservoir at the entry point with a near horizontal inclination, and remaining in the reservoir until the desired bottom hole location is reached (Helms 2013). This type of wellbore is considered more economically successful in thin reservoirs as more of the wellbore is significantly exposed to the reservoir as compared to a vertical well penetrating the reservoir perpendicularly as shown in Figure 9.

Slant drilling is drilling at an angle from the vertical usually $30° - 45°$. Surface environmental disturbances are minimized applying this type of drilling technique. For example, using the slant drilling method onshore to tap oil and gas reserves under a lake. (Heavy Oil Science Center 2013)
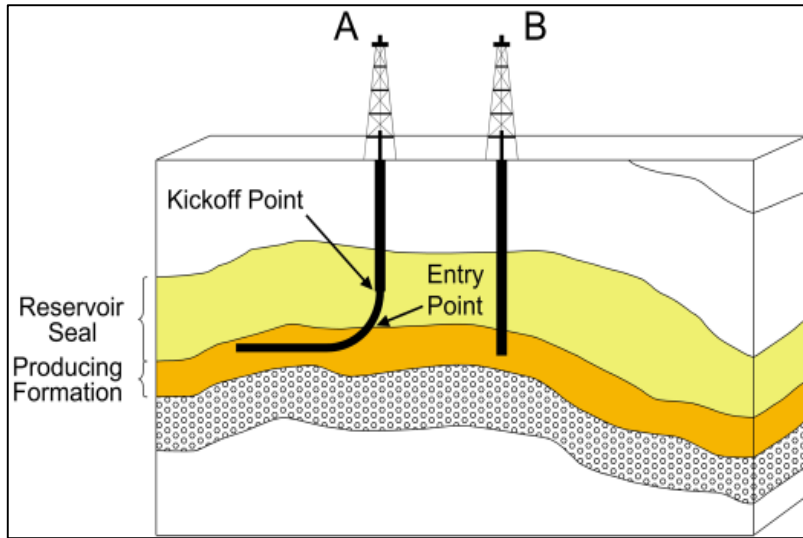
Figure 9: Length of producing formation exposed to the wellbore

(Helms 2013)

Similarly, pipelines range in angles from horizontal, inclined to vertical. The most common in field pipelines being horizontal and inclined pipeline configurations. A horizontal and inclined pipeline consists of three different sections: horizontal, upward inclined and downward inclined section. (Bagci and Al-Shareef 2003)

2.4 Nature of Produced Sand and Fines

Sands are basically detrital grains of mineral oxides (i.e. SiO_2), and fines (clay) are hydrous aluminum silicates that may be detrital or authigenic. Sand particles are the load-bearing solids of a formation while fines are not part of the mechanical

structure. (Rawlins and Hewett, 2007). The properties for sand and fines are shown in Table A 1 (Appendix).

The percentage of fines in a rock is commonly used as one of the key parameters for sand control type selection. One of the key design criteria in sand control is to allow the fines present to move through whilst holding back the sand. Although different definitions of fines seem to exist and some arbitrary size and/or compositional definitions are often used which could lead to an inappropriate sand control design. (Byrne et al. 2010)

The Wentworth scale for classification of rocks is shown in Table A 2 (Appendix). Byrne, et al. (2010) did state 45 microns as being the generally accepted maximum value for fines as far as engineering is concerned, i.e. fines should be less than 45 microns. However this definition might only be appropriate for specific type of reservoirs, thus the preferred definition of fines is given as that part of a rock that can move through the pores of the undisturbed intact rock.

CHAPTER 3
MULTIPHASE FLOW PATTERNS

The production and transportation of multiphase gas-liquid-solid is a common trend in the petroleum industry, as sand is most often produced along with reservoir fluids. Multiphase fluid flow is considered a transient phenomenon since the flow pattern changes, from dispersed bubble to slug, plug, annular and stratified flow patterns depending on the flow rates, fluid properties, pipe size, topography and corresponding pressure drop (Bello et al. 2011). Figure 10 and Figure 11 show the flow patterns in horizontal and vertical pipes respectively. The addition of a gaseous phase to an oil-water flow increases the pressure drop and induces disturbances and instabilities caused by gas bubbles, plugs and slugs especially for the most favorable flow patterns such as core annular flow (Sotgia 2006). Sotgia (2006) gave an expression for pressure drop reduction factor in a three-phase oil-water-gas flow, R_{3P} as,

$$R_{3P} = \Delta p_{o-w} \Big/ \Delta p_{o-w-g}$$

[3-1]

Δp_{o-w} = Pressure drop of oil-water flow

Δp_{o-w-g} = Pressure drop of oil-water-gas mixture

Pressure drop is discussed later in this chapter (Page 33).

3.1 Two-Phase Flow Patterns in Horizontal Pipes

In a two-phase, gas-liquid flow, where the liquid is much more than the gas, little amounts of tiny gas bubbles could be seen in the liquid (bubble flow), which may eventually mix with the liquid if the liquid flows fast enough to create sufficient turbulence. In another instance, where the gas is more, it could carry little amounts of liquid droplets, which becomes deposited on the pipe wall and flows in the form of a thin film on the pipe wall. This type of flow is referred to as annular flow. (Bratland 2010). Flow patterns in horizontal two-phase gas-liquid flow is illustrated in Figure 10.

Stratified smooth flow is common in horizontal flow with relatively low gas and liquid flow rates. When the gas flow rate is increased, waves begin to generate in the pipe (stratified wavy flow) and could reach the top of the pipe. As the gas gets confined in the pipe, the flow tends to be discontinuous, resulting in the formation of slugs or elongated bubbles. (Bratland 2010).
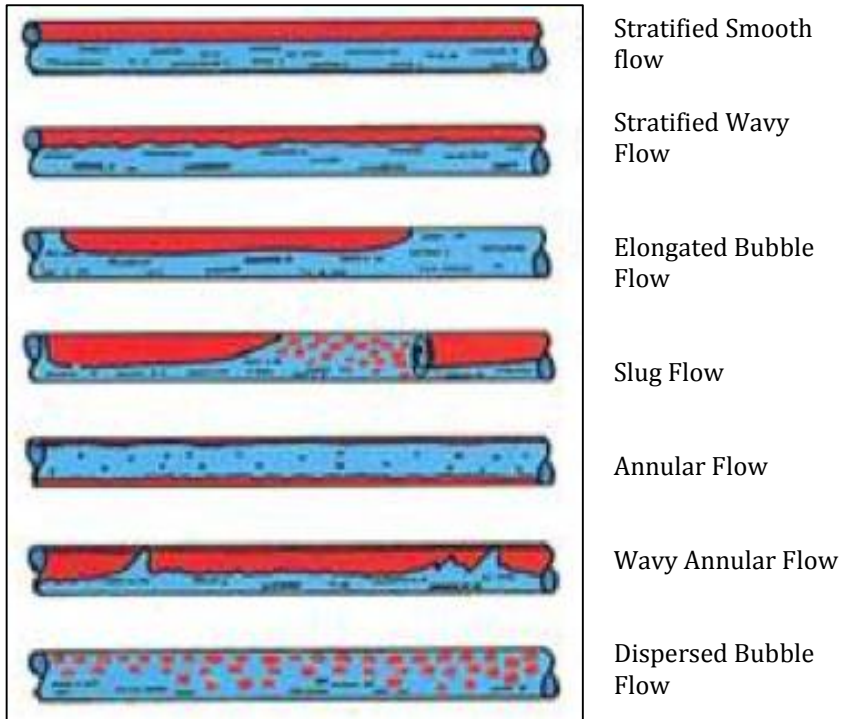
Figure 10: Flow patterns in horizontal pipe (Bello et al. 2011)

3.2 Two-Phase Flow Pattern in Vertical Pipes

Normally the denser fluid of the two settles at the base in a horizontal pipe, but there is no opportunity for such in a vertical pipe, hence stratified flow is impossible in vertical pipes (Bratland 2010).
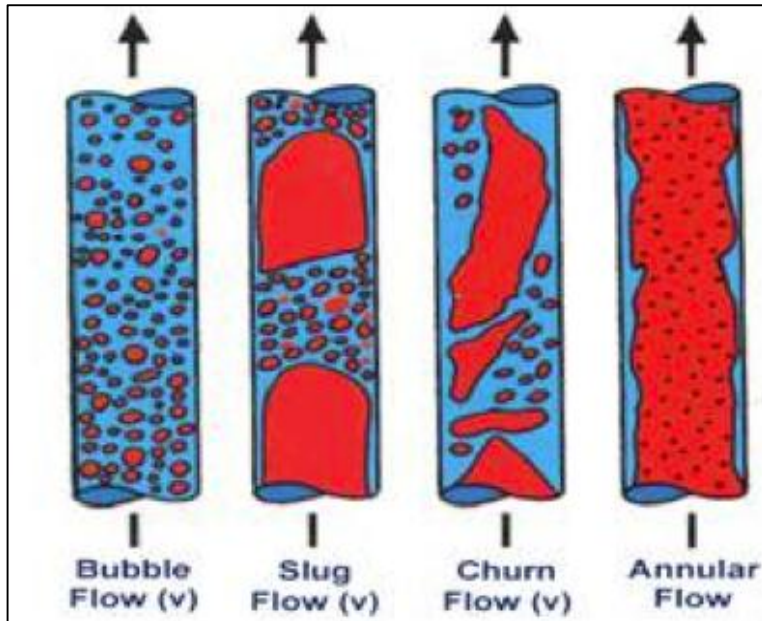
Figure 11: Flow patterns in vertical pipe (Bello et al. 2011)

3.3 Two-Phase Flow Pattern Map

The flow pattern map is a diagram used to display transition boundaries between flow patterns usually presented on a log-log graph whose axes represent velocities of the two phases. One of the most widely quoted flow pattern maps for vertical upflow and horizontal flow are those of Fair (1960) and Baker (1954) respectively (Thome 2010).

The value of the mass velocity, $\dot{m}$, has to be known and x-axis must be calculated to be able to apply the Fair (1960) flow pattern map illustrated in Figure 12. The intersection of the two values on the map determines if the flow falls under bubble, slug annular or

mist flow. The transition thresholds between the flow patterns are indicated with the dark lines. (Thome 2010)
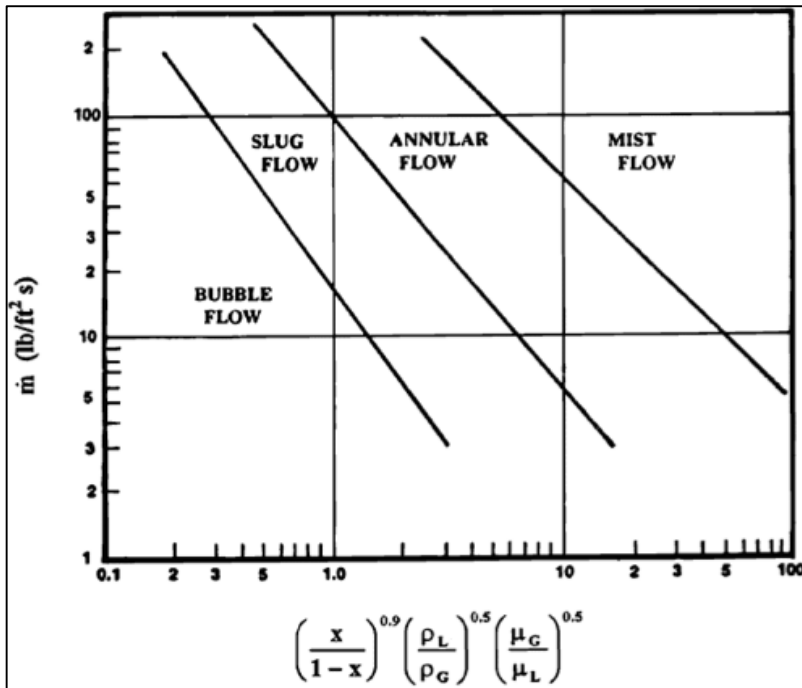
Figure 12: Fair (1960) two-phase flow pattern map for vertical upward flow (Thome 2010)

To use the Baker (1954) map to determine flow patterns, the mass velocities of gas and liquid has to be determined. The gas-phase parameter, λ and liquid-phase parameter, Ψ is calculated using the equations below:

$$\lambda = \left(\frac{\rho_G}{\rho_{air}} \frac{\rho_L}{\rho_{water}}\right)^{1/2}$$

[3-2]

28

$$\Psi = \left(\frac{\sigma_{water}}{\sigma}\right)\left[\left(\frac{\mu_L}{\mu_{water}}\right)\left(\frac{\rho_{water}}{\rho_L}\right)^2\right]^{1/3}$$

<div align="right">[3-3]</div>
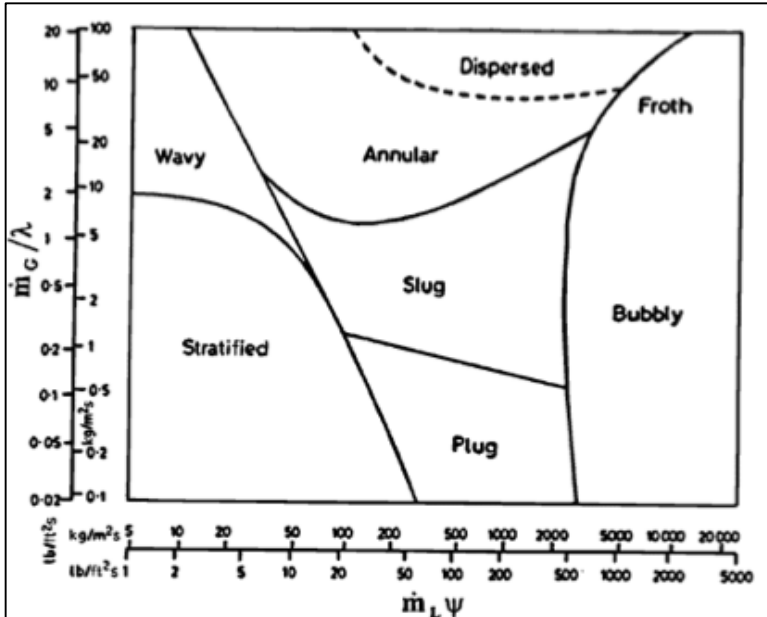
Figure 13: Baker (1954) two-phase flow pattern map for horizontal flow (Thome 2010)

3.4 Three-Phase Flow Patterns

This thesis work is focused on multiphase gas-liquid-solid flow in petroleum industry. Illustrating a flow regime for a three-phase flow is quite difficult compared to two-phase flow, as some authors have tried but ended up with very complicated illustrations of limited validity (Bratland 2010). A more convenient way of illustrating the three-phase flow is shown in Figure 14.

Possible two-phase flow patterns is shown on the borders i.e. gas-oil in left border, gas-water, right border and oil-water lower border. Many more flow regimes exist when all phases are present simultaneously. Operation points inside the triangle will indicate three-phase flow. The gas superficial velocity as a fraction of the total superficial velocities is seen on the vertical axis of the three dimensional triangle, and is equal to 1 for a pure gas flow. (Bratland 2010). Similar trend goes for other axis.

As earlier mentioned in this work, the two major types of interactions as far as fluid dynamics is concerned are: interphase interaction, where the fluid phase interacts with the particulate phase, and intraphase interaction, where solid particles interact with each other (Doan et al. 1993).
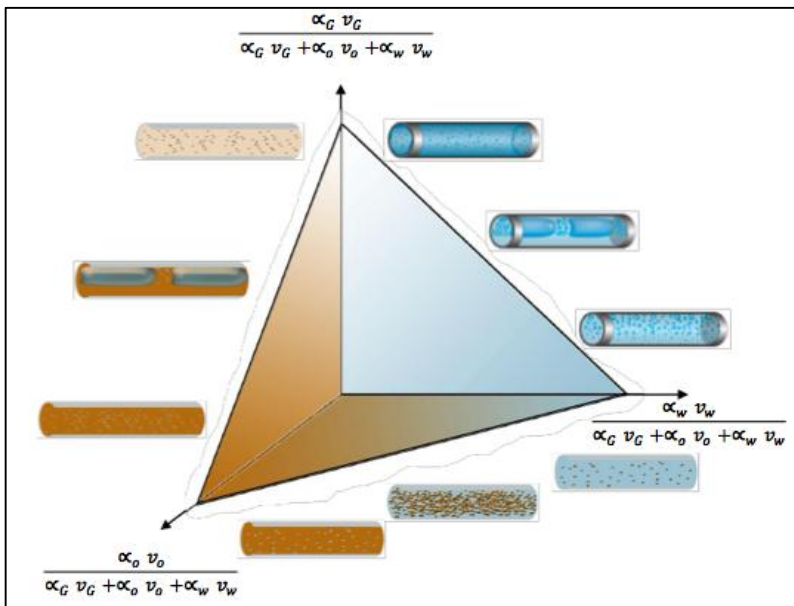
Figure 14: Three-phase gas-oil-water diagram for horizontal pipes (Bratland 2010)

3.5 Prediction of Flow Regime

It is imperative to pay attention to the flow regime as it has a huge impact on the sand carrying capacity of the flow (Danielson 2007). Beggs and Brill (1973) method is applied in gas-liquid flow regime for horizontal and/or vertical flow (Bello 2008). The following expressions are used for the prediction:

$$N_{Fr} = v_{2m}^2 \big/ gD$$

[3-4]

$$\lambda_L = q_L \big/ q_L + q_g$$

[3-5]

$$L_1 = 316\lambda_L^{0.302}$$

[3-6]

$$L_2 = 0.0009252\lambda_L^{-2.4684}$$

[3-7]

$$L_3 = 0.10\lambda_L^{-1.4516}$$

[3-8]

$$L_4 = 0.50\lambda_L^{-6.738}$$

[3-9]

Flow is segregated (annular or stratified) when,

$$\lambda_L < 0.01 \ and \ N_{Fr} < L_1 \ or \ \lambda_L \geq 0.01 \ and \ N_{Fr} < L_2$$

[3-10]

Flow is intermittent (slug) when,

$$0.01 \leq \lambda_L < 0.4 \ and \ L_3 < N_{Fr} \leq L_1 \ or \ \lambda_L \geq 0.4 \ and \ L_3 < N_{Fr}$$
$$\leq L_4$$

[3-11]

Flow is distributed (bubble or dispersed) when,

$$\lambda_L < 0.4 \ and \ N_{Fr} \geq L_1 \ or \ \lambda_L \geq 0.4 \ and \ N_{Fr} > L_4$$

[3-12]

Flow is transition when,

$$\lambda_L \geq 0.01 \ and \ L_2 < N_{Fr} \leq L_3$$

[3-13]

3.6 Two-Phase Pressure Drop: Lockhart-Martinelli Method

Lockhart and Martinelli in 1949, proposed a correlation method for two-phase flow in pipes, based on the assumption that the static pressure drop for the liquid and gas phase flowing at the same time is equal at any point in the pipe (Muzychka and Awad 2010).

3.6.1 Static Head Loss

The static head loss is necessary when dealing with vertical flow.

$$\Delta P_s = \frac{g}{g_c} \int \rho_{tp} dH \sin \theta$$

[3-14]

$\sin \theta = 1$ for vertical units

ρ_{tp} can vary with height, H, and is expressed as

$$\rho_{tp} = R_G \rho_G + (1 - R_G)\rho_L$$

[3-15]

Martinelli relationship is used to express the volume fraction of gas, R_G as

$$R_G = 1 - \frac{1}{\Phi_L} = 1 - R_L$$

[3-16]

Φ_L is defined in section 3.5.3

3.6.2 Momentum Head Loss

The momentum head loss is easily determined from the inlet and outlet conditions given as

$$\Delta P_m = \frac{G_t^2}{g_c} \left\{ \left[\frac{(1-x)^2}{\rho_L(1-R_G)} + \frac{x^2}{\rho_G R_G} \right]_2 - \left[\frac{(1-x)^2}{\rho_L(1-R_G)} + \frac{x^2}{\rho_G R_G} \right]_1 \right\}$$

[3-17]

x = local weight fraction of vapor

(Bell and Mueller 2001)

3.6.3 Frictional Head Loss

The single-phase pressure drop is expressed as:

$$\Delta P_L = 4f_L(L/d_i)G_t^2(1-x)^2(1/2g_c\rho_L)$$

[3-18]

$$\Delta P_G = 4f_G(L/d_i)G_t^2 x^2(1/2g_c\rho_G)$$

[3-19]

34

The two-phase frictional pressure drop based on two-phase multiplier for the liquid-phase or vapor-phase is given as:

$$\Delta P_f = \Phi_L^2 \Delta P_L$$

[3-20]

$$\Delta P_f = \Phi_G^2 \Delta P_G$$

[3-21]

The two-phase multipliers are expressed as:

$$\Phi_L^2 = 1 + C/X + 1/X^2, \text{ for } Re_L > 4000$$

[3-22]

$$\Phi_G^2 = 1 + CX + X^2, \text{ for } Re_L < 4000$$

[3-23]

The value of C is dependent on the liquid and gas regime, which is 20 when both phases are in the turbulent regime.
The Martinelli parameter for both phases in the turbulent regime is expressed as:

$$X = \left(\frac{1-x}{x}\right)^{0.9} \left(\frac{\rho_G}{\rho_L}\right)^{0.5} \left(\frac{\mu_L}{\mu_G}\right)^{0.1}$$

[3-24]

(Thome 2010)

3.7 Three-Phase Pressure Drop

The total pressure gradient in a three-phase solid-liquid-gas flow is expressed as:

$$\left(\frac{dP}{dl}\right)_{tot} = \left(\frac{dP}{dl}\right)_f + \left(\frac{dP}{dl}\right)_s$$

[3-25]

Where subscripts f and s signifies fluid flow and solid transport in fluid flow respectively.

3.7.1 Fluid Flow Pressure Gradient

Adeyanju and Oyekunle (2012), quoted the Giles et al (2009) equation,

$$\frac{dp}{\gamma} + \frac{vdv}{g} + dxsin\theta + dh_1 = 0$$

[3-26]

h_1 is obtained from Darcy-Weisbach equation as,

$$h_1 = \frac{f_1 v^2}{2gd}$$

[3-27]

The wall friction f, is given as,

$$f = \frac{2\tau_f}{V^2 \rho_f}$$

Where,

ρ_f is the fluid (oil and gas) density.

The continuity equation for compressible fluid flow in pipe is given as,

$$m = A\gamma v$$

Where,

$$\gamma = \frac{1}{\rho_f}$$

Inserting equations [3-26] and [3-27] into derivatives of equation [3-29],

$$\frac{dp}{dl} = \frac{\frac{fm^2}{2A^2\gamma dg} + \gamma \sin\theta}{1 - \frac{m^2}{\gamma^2 A^2 g}\frac{d\gamma}{dp}}$$

Compressibility of reservoir fluids is expressed as:

$$C_f = \frac{1}{\gamma}\frac{d\gamma}{dp}$$

[3-32]

Inserting equation [3-32] in equation [3-31]:

$$\left(\frac{dp}{dl}\right)_f = \frac{\dfrac{fm^2}{2A^2\gamma dg} + \gamma\sin\theta}{1 - \dfrac{m^2 C_f}{\gamma A^2 g}}$$

[3-33]

3.7.2 Pressure Gradient due to Solid Transport in Fluid Flow

Conservation equation for solid phase is given as:

$$\frac{\partial(\rho_P)}{\partial t} + \frac{\partial(\rho_P v_P)}{\partial x} = 0$$

[3-34]

Momentum equation for solid phase is given as:

$$\frac{\partial(\rho_P v_P)}{\partial t} + \frac{\partial(\rho_P v_P^2)}{\partial x} = \sum_{i=1}^{6} F_i$$

[3-35]

Assuming a constant solid density and neglecting the acceleration term, equation [3-35] reduces to:

$$\rho_P \frac{dv_P}{dt} = \sum_{i=1}^{6} F_i$$

[3-36]

Where

ρ_P = Particle density

F_i = Force per unit volume

Multiplying equation [3-34] with solid volume, gives

$$m_P \frac{dv_P}{dt} = F_M + F_B + F_P - F_V - F_D - F_G$$

[3-37]

Where

m_P = Mass of particle

The forces are described in section 3.8 and illustrated in Figure 15.

$$m_P = \frac{\pi}{6} d_P^3 \rho_P$$

[3-38]

For a fully developed flow

$$\frac{dv_P}{dt} = v_P \frac{dv_P}{dx}$$

<div align="right">[3-39]</div>

Inserting equation [3-39] and [3-38] in [3-37] gives,

$$\left(\frac{dP}{dl}\right)_s = v_P \frac{\pi}{6} d_P^3 \rho_s \frac{dv_s}{dx} = F_M + F_B + F_P - F_V - F_D - F_G$$

<div align="right">[3-40]</div>

The ratio of upward force to downward force on sand particles can be expressed as:

$$k = \frac{F_M + F_B + F_P}{F_V + F_D + F_G}$$

<div align="right">[3-41]</div>

This implies that if k is less than 1, sand particles will deposit at the base of the tubing.

Ling et al. (2012) derived governing equations for gas-oil-water three-phase turbulent and laminar flow in pipe, under the assumption of steady state flow condition. The pressure drop for turbulent flow is given as:

$$\frac{dp_f}{dl} = \frac{0.028 \left[\left(\frac{\mu_g}{A_g}\right)^{0.25} \rho_g^{0.75} \bar{v}_g^{1.75} S_g^{1.25} + \left(\frac{\mu_o}{A_o}\right)^{0.25} \rho_o^{0.75} \bar{v}_o^{1.75} S_o^{1.25} + \left(\frac{\mu_w}{A_w}\right)^{0.25} \rho_w^{0.75} \bar{v}_w^{1.75} S_w^{1.25} \right]}{A_g + A_o + A_w}$$

[3-42]

The pressure drop for laminar flow is given as:

$$\frac{dp_f}{dl} = \frac{2 \left(\frac{\mu_g \bar{v}_g}{A_g} S_g^2 + \frac{\mu_o \bar{v}_o}{A_o} S_o^2 + \frac{\mu_w \bar{v}_w}{A_w} S_w^2 \right)}{A_g + A_o + A_w}$$

[3-43]

Where

$\bar{v}_g$, $\bar{v}_o$ and $\bar{v}_w$ are average velocities for gas, oil and water respectively

S_g, S_o and S_w are perimeter length of gas, oil, and water contacted with pipe wall respectively

A_g, A_o and A_w are cross-sectional area of gas, oil and water phase respectively

3.8 Forces Acting on a Particle in a Gas-Liquid-Solid Multiphase Flow
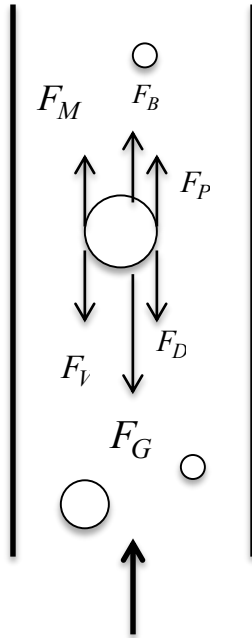
Fluid flow direction (inside the tubing)

Figure 15: Forces acting on a solid particle in a multiphase flow (Adeyanju and Oyekunle 2012)

Particle-Particle Interaction Force (F_P)

The expression for particle-particle interaction force in gas-liquid-solid multiphase pipe flow is given as:

$$F_P = \frac{\pi}{4} d_P^2 \frac{m_s}{A} (v_M - v_P)$$

<div align="right">[3-44]</div>

Where,

d_P = Solid particle diameter

m_s = Input solid-phase mass flow rate or sand mass production rate into the wellbore or pipeline.

A = Cross-sectional area of pipe

$v_M - v_p$= Particle slip velocity between solid and fluid (gas-liquid) mixture.

$$v_M = v_G + v_L$$

<div align="right">[3-45]</div>

Particle-Liquid Transferred Force (F_M)

This force is as a result of linear momentum transferred between the fluid phase and the sand phase, expressed as:

$$F_M = \frac{F^{\wedge} \left(\frac{qu}{2a^2 \rho_P} \right)}{\left[1 + \left(\frac{\bar{\rho}_L}{2\bar{\rho}_P} \right) \right]}$$

<div align="right">[3-46]</div>

Where,

$$a = \frac{d_P}{2} = \text{Sand particle radius}$$

$$F^\wedge = \frac{C_D}{24}\left[\frac{2a\rho_L(v_L - v_P)}{\mu}\right]$$

<div align="right">[3-47]</div>

Viscous Force, (F_V)

Stokes Law is used to express the viscous force on a spherical sand particle in a flowing fluid.

$$F_v = 3\pi\mu d_P(v_M - v_P)$$

<div align="right">[3-48]</div>

Buoyancy Force, (F_B)

The buoyancy force in a gas-liquid-solid three-phase pipe flow is expressed as:

$$F_B = \frac{1}{6}\pi d_P^3 \rho_M g$$

<div align="right">[3-49]</div>

Where,

$g = \text{Gravitational acceleration}$

ρ_M = Gas-liquid mixture density

$$\rho_M = \rho_G H_G + \rho_L (1 - H_G)$$

[3-50]

Gravity Force, (F_G)

The expression for gravity force is similar to that for buoyancy force, with the fluid density (ρ_f) replaced by particle density (ρ_P). It is given as:

$$F_G = \frac{1}{6}\pi d_P^3 \rho_P g$$

[3-51]

Frictional Drag Force, (F_D)

The expression for drag force on a single suspended particle from a liquid phase is given as:

$$F_D = \alpha(v_M - v_P)$$

[3-52]

$$\alpha = C_D \rho_f \frac{v_M - v_P}{2} \frac{(\pi d_P^2)}{4}$$

[3-53]

Where,

α= Momentum transfer coefficient

C_D= Drag coefficient (dependent on Reynolds number)

Expressions for drag coefficient in the three various regions
(Stokes law, transition, and Newton law region) are shown in
Table A 3 (Appendix).

Particle Reynolds number (Re_p) is expressed as

$$Re_P = \frac{\rho_f v_P d_P}{\mu_f}$$

[3-54]

(Adeyanju and Oyekunle, 2012 and Bello, 2008)

CHAPTER 4
SAND MANAGEMENT

In a bid to control cost associated with sand production, the petroleum industry has drifted from the traditional sand control to what is termed sand management (Mathis 2003). Sand management is an operating concept where traditional sand control means are not normally applied, and production is maximized and maintained through monitoring and control of fluid rates, well pressures and sand inflow. Sand control involves high cost and low risk solutions while sand management represents low costs solutions but active risk management (Tronvoll , et al. 2001). Over 70% of the world's oil and gas fields employ sand management when making field development decisions (Sereneworld 2013).

Knowing the reasons behind sand production from a reservoir and/or being able to predict sand production is always the first right step to take towards sand management. The cause of sand production usually either has to do shear failure of the rock matrix due to pressure depletion or tensile failure of the individual sand particle disintegrated from the parent rock as a result of fluid flow through the rock matrix (McKay et al. 2008).

4.1 Prediction of Sand and Fines Production

It is difficult to successfully predict sand production in a wells' exploitation phase using only one method of prediction. Hence

several methods are considered to achieve optimal prediction accuracy (Hong'en et al. 2005). Hong'en, et al. (2005) described five empirical methods of predicting sand production: interval transit-time method, combination modulus method, Schlumberger method, porosity method and bottom-hole pressure control method.

4.1.1 Interval Transit-Time Method

Forecast of sand production can be done using acoustic logging data of formation. A critical interval transit-time value, 295 $\mu s/m$ is defined, such that if Δt is more than this value, then the well is most likely going to produce sand and vice-versa. However this value is slightly different for different oil fields.

4.1.2 Combination Modulus Method

Numerous analyses on statistical results of oil well sand production show that no sand is produced when elastic combination modulus, E_C is more than or equal to 2.88×10^6 psi, light sand is produced when E_C is between 2.16×10^6 psi and 2.88×10^6 psi, and great sand is produced when E_C is less than 2.16×10^6 psi. E_C is calculated from the equation:

$$E_C = \frac{9.94 \times 10^8 \times \rho}{\Delta t_c^2}$$

[4-1]

ρ = Layer density

Δt_c^2 = Time difference of sound wave

4.1.3 Schlumberger Method

In the Schlumberger method, $E_S \times E_B$ is calculated. It is a function rock porosity, Poisson ratio and interval transit time. It is suggested that no sand is produced when $E_S \times E_B$ is more than $5.51 \times 10^9 \ psi$ and sand is possibly produced when $E_S \times E_B$ is less than $4.79 \times 10^9 \ psi$. $E_S \times E_B$ is expressed as:

$$E_S \times E_B = \frac{(9.94 \times 10^8)^2 (1 - 2\mu)(1 + \mu)\rho^2}{6(1 - \mu)^2 (\Delta t_c)^4}$$

[4-2]

4.1.4 Porosity Method

The porosity of a formation could also be a determining factor in deciding if sand production will occur or not. The possibility of sand production is higher if porosity exceeds 30%. Slight sand production could happen for porosity within the range of 20% to 30%.

4.1.5 Bottom-hole Pressure Control Method

Researchers of former Soviet Union put forward bottom-hole pressure control method and proposed that formation stability near wellbore is related with not only formation properties but also bottom-hole pressure. This is based on conditions that

tangential stress on bottom formation is less than cementing force of the rock particle in order to prevent sand production. They deduced an equation of bottom-hole flowing pressure to prevent sand production as follow:

$$P_{wf} \geq \rho g H \beta (\cos \theta) \left(\frac{2\mu}{1 - \mu} - a \right) \times 10^3 - C$$

[4-3]

β = Rock pressure conductor coefficient

θ = Formation slant angle

C = Particle Cohesion

a = Particle friction force coefficient

An example of how some of these parameters change with depth can be seen in Figure 14.
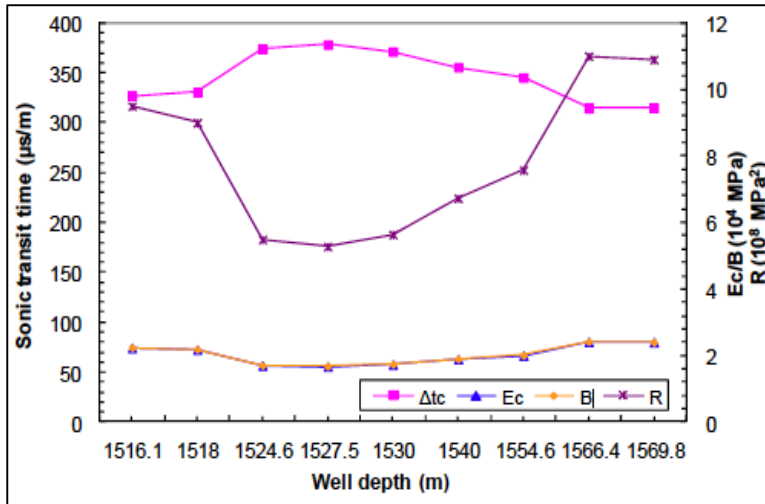
Figure 16: Sanding prediction curve (Luo et al. 2012)

4.2 Sand and Fines Transport in Tubing (Vertical Flow)

In a vertical flow, the solid particles settle in a direction parallel to the average direction of motion of the liquid-solid flow. Thus, collision between particles and wall are very much less frequent than is experienced in horizontal pipelines. (King 2002). Solid particles can be conveyed upward when the transport condition is well satisfied, which is true when the fluid velocity exceeds the terminal settling velocity of the solid particle. (Weber 2012).

The ratio of the mean velocity of fluid flow to settling velocity of solid particles can be used to determine the ability of the fluid flow to move particles along in the tubing (Mazurek, et al. 2002).

$$\lambda = v/w$$

[4-4]

Where

v = Mean velocity of flow

w = Settling velocity of mean sized particles

Sand and fines will settle down through the fluid quicker than the flow can carry the particles if λ is very small and vice versa.

Bello et al. (2011) gave the minimum transport velocity (v_t) in a vertical multiphase pipe flow as:

$$v_t = A * \left[\frac{g d_P (\rho_P - \rho_M)}{C_D \rho_M}\right]^B$$

[4-5]

Constants A and B are defined in Table A 5 (Appendix)

4.3 Sand and Fines Transport in Pipelines (Horizontal Flow)

Similarly as in the vertical flow, the fluid velocity has to remain high enough (higher than the MTV) to ensure the continuous movement of solid particles and prevent the formation of sand bed in the pipe base. Several correlations have been developed to explain solid transport in multiphase flow but ended up generalizing liquid-sand models to gas-liquid-sand models. (Danielson 2007).

Danielson (2007) developed the Drift-Flux model to properly address the issues of solid transport in multiphase flow and predict minimum transport velocity in pipelines. The drift flux model assumes the gas velocity as a linear function of the mixture velocity, over a wide range of conditions. The gas velocity (v_G) is expressed as:

$$v_G = Cv_M + v_O$$

[4-6]

Where,

v_M = Mixture velocity

$C \cong 1.2$ for air/water.

v_O = Bubble rise velocity, which is given as:

$$v_O = 0.4\big((\rho_L - \rho_G)/\rho_L\big)^{1/2}(gD)^{1/2}$$

[4-7]

Where,

ρ_L & ρ_G = Liquid and Gas density

The expression for gas velocity in terms of superficial gas velocity (v_{SG}) and liquid hold up (H_L) is given as:

$$v_G = v_{SG}/(1 - H_L)$$

[4-8]

The liquid hold-up (H_L) is given as:

$$H_L = 1 - v_{SG}/v_G$$

[4-9a]

$$H_L = 1 - v_{SG}/(Cv_M + v_O)$$

[4-9b]

The liquid velocity (v_L) can be calculated after liquid hold-up is known using:

$$v_L = v_{SL}/H_L$$

[4-10]

Where,

v_{SL}= Superficial liquid velocity

The influence of increased gas velocity on solid particles is indirect, as it only directly impacts the liquid where the result is a higher fluid velocity, which in turn reduces the sand hold-up.

The overall hold-up (H_O), is expressed as:

$$H_O = H_L + H_S$$

[4-11]

Where

H_S= Sand hold-up

The minimum transport velocity is given as:

$$v_t = v_L - v_S$$

[4-12a]

$$v_t = {v_{SL}}/{H_L} - {v_{SS}}/{H_S}$$

[4-12b]

$$v_t = {v_{SL}}/{(H_O - H_S)} - {v_{SS}}/{H_S}$$

[4-12c]

This equation finally results in:

$$v_t H_S^2 + (v_{SL} + v_{SS} - v_t H_O)H_S - v_{ss}H_O = 0$$

[4-13]

Where,

v_S = Sand velocity

v_{SS} = Sand superficial velocity

During normal case scenario of sand production, the ratio v_{SS}:v_{SL} will be at 1:5000, while v_{SG}:v_{SL} will be 1:1 for slug flow. Using these assumed ratios for typical sand production rates, the drift-flux model can be used to calculate the overall hold-up, sand hold-up and the MTV. (Danielson 2007).

Bello et al. (2011) developed a velocity profile model for multiphase flow in a horizontal pipe, given as:

$$V_R = A * f * Re^B * \left[1 - \left(\frac{r}{R}\right)^2\right]^C$$

<div align="right">[4-14]</div>

Where,

V_R= Velocity of fluid particle at a particular point in the pipe cross-section

f = Friction factor

r = Distance from the pipeline center to any point

R = Pipe radius

Constants A, B and C are defined in Table A 4 (Appendix)

Gregory, et al. (1978) developed a model for liquid hold-up in slug flow (Maley and Jepson 1998). It is given as:

$$H_L = 1 \Big/ 1 + \left(\frac{v_M}{8.66}\right)^{1.39}$$

<div align="right">[4-15]</div>

4.4 Sand Erosion in Multiphase Flow

Erosion caused by sand particles in multiphase flow is a more complex phenomenon as compared to single-phase flow. This is due to the different flow regimes present in multiphase flow (McLaury et al. 2010). The American Petroleum Institute

Recommended Practice 14E (API RP 14E) in 1991, came up with an empirical equation for erosional velocity (v_e):

$$v_e = {C} \Big/ {\sqrt{\rho_M}}$$

[4-16]

Where,

ρ_M = Fluid mixture density

C = Empirical constant (100 for continuous and 125 for intermittent service in solids-free fluids)

(Odigie, et al. 2012)

Erosion in pipes is dependent on several elements which include, particle impact speed, angle of impact, sharpness and concentration of sand, fluid properties (e.g. viscosity), fluid velocities etc. The above equation (equation [4-15]) failed to take into consideration key parameters such as fluid properties, sand size, sand production rate, Reynolds number etc. Hence, many researchers have over the years tried to develop models that will encompass these missing factors. These include works from Salama (1998) and McLaury and Shirazi (2000). (Odigie, et al. 2012).

Challenges are already associated with the transport of two-phase gas-liquid. The inclusion of solids to the flow increase concerns and poses more challenges. The effect of sand erosion is felt more in a gas dominant multiphase flow system. Reasons being

that more of gas makes the system lighter (lower fluid density), hence will have a higher flow velocity accompanied with more solid impingements of wall surfaces. Annular and slug flow are the only two multiphase flows with considerable amount of gas to result in severe erosion. (McLaury, et al. 2010).

McLaury, et al. (2010) developed a mechanical model for predicting sand erosion rate in three-phase gas-liquid-solid flow, focusing on annular and slug flow. It was noted that the most important parameter in the prediction of sand erosion is the particle impact velocity.

4.4.1 Mechanistic Erosion Model for Annular Flow
For the annular flow, which contains considerable amount of gas in the core with high velocities and low-velocity liquid film around the walls of the pipe with small droplets in the core, the entrainment fraction E, for vertical flow is given as:

$$\frac{E}{1-E} = 0.003 We_{SG}^{1.8} Fr_{SG}^{-0.92} Re_{SG}^{-1.24} Re_{SL}^{0.7} \left(\frac{\rho_L}{\rho_G}\right)^{0.38} \left(\frac{\mu_L}{\mu_G}\right)^{0.97}$$

[4-17]

$We_{SG}, Fr_{SG}, Re_{SG},$ and Re_{SL} are dimensionless parameters given as:

$$We_{SG} = \rho_G v_{SG}^2 d_p \Big/ \sigma$$

[4-18]

$$Fr_{SG} = v_{SG} \Big/ \sqrt{gd_p}$$

$$[4\text{-}19]$$

$$Re_{SG} = \rho_G v_{SG} d_p \Big/ \mu_G$$

$$[4\text{-}20]$$

$$Re_{SL} = \rho_L v_{SL} d_p \Big/ \mu_L$$

$$[4\text{-}21]$$

Where,

σ = Surface tension

Particle impact velocity for particles in the gas core flowing with liquid droplets, is assumed to be same as average velocity of gas in the gas core, and is expressed as:

$$v_G = v_{SG} \left[d_p \Big/ d_p - 2\delta \right]^2$$

$$[4\text{-}22]$$

Where,

δ = Liquid film thickness

For particles in the liquid film, the impact velocity is given as:

$$v_F = v_{SL}\,(1 - E)d_p^2/4\delta(d_p - \delta)$$

[4-23]

4.4.2 Mechanistic Erosion Model for Slug Flow

In slug flow, there exist a higher liquid velocity as compared to annular flow regime. For successful erosion prediction in slug flow, the fraction of liquid in slug body must be known, and it is given as:

$$Fraction\ of\ liquid\ in\ slug\ body$$
$$= {L_{LS}H_{LS}v_{LS}}/{L_{LS}H_{LS}v_{LS}} + L_F H_F v_F$$

[4-24]

Where,

L_{LS} = Length of liquid slug body

H_{LS} = Liquid hold-up fraction in slug body

v_{LS} = Velocity of liquid slug body

L_F = Length of liquid film

H_F = Liquid hold-up fraction in liquid film

v_F = Velocity of liquid film

- Sand flows with liquid
- Fractions of particles in the liquid slug body is equal to the fraction of liquid in the liquid slug body
- Sand particles are distributed homogeneously in the liquid slug body

For slug flow, the total penetration caused by particle impact is determined using equation [4-23].

$$P_{total} = P_{FS}\left(L_{FS}/L_{FS} + L_{RS}\right) + P_{RS}\left(L_{RS}/L_{FS} + L_{RS}\right)$$

[4-25]

Where,

P = Penetration rate

Subscripts FS and RS = Front and remainder of the liquid slug respectively

(McLaury et al. 2010).

4.5 Detection of Sand and Fines in Pipelines

It is the desire of every oil company to be able to successfully control and manage produced sand at minimum cost while optimizing oil and gas production. Early detection of sand and fines flowing through pipes is key to oil and gas production optimization, as erosion is predicted more accurately and

production rates will not have to be unnecessarily limited.
(Odigie, et al. 2012)

Most of the sand detectors or monitoring instrument in the oil and
gas industry are based on the measurement of erosion or
ultrasonic signals produced by particle impacts on pipe walls.
(Nabipour, et al. 2012).

Nabipour et al. (2012) gives an insight to the most common sand
monitors and further looked at how to improve data quality and
interpretation through the integration of available techniques for
sand monitoring. The available techniques could be classified
based on their location as:

Intrusive

- ER Probes
- Intrusive Acoustic Probes

Non-Intrusive

- Clamp-On Ultrasonic Detectors

Ultrasonic Detectors
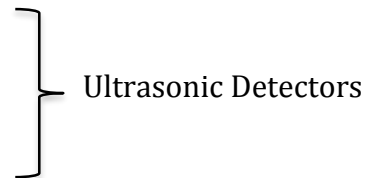
4.5.1 ER Probes

The ER probes are erosion-based detectors, consisting of intrusive
probes, which have on it sensing elements and are always placed
inside the pipe. Erosion is observed on the probe overtime due to
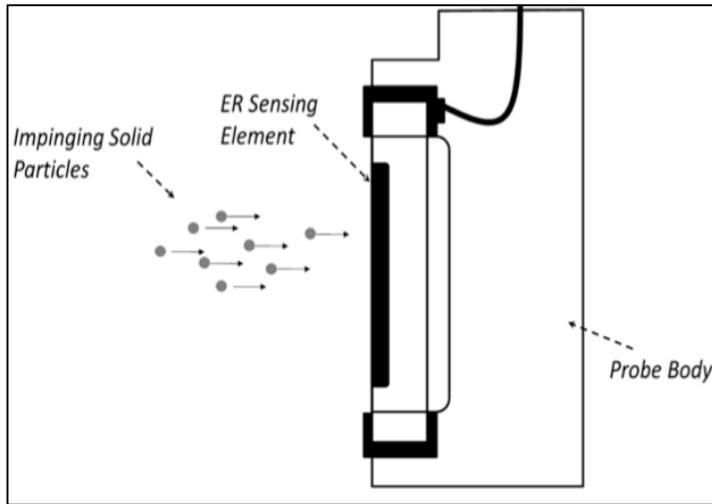particle impacts on the sensing elements as seen in Figure 15.

Figure 17: Schematic of ER Probe (Nabipour, et al. 2012)

The wall thickness of the sensing element eroded can be determined by measuring the electrical resistance (ER) of the sensing element over a period of time. After which some empirical equations are used to link the amount of thickness reduction to the amount of sand produced.

In other words, the precision of the empirical equation recommended by the manufacturer is the determining factor of the effectiveness of this method for sand detection in pipes. However, it has been proven by researchers that the ER probes are quite useful in determining cumulative sand production but do not estimate instantaneous sand production.

4.5.2 Intrusive Acoustic Probes

The intrusive acoustic probes are ultrasonic-based detectors, which record converted ultrasonic signals (in electrical form)

generated from particle impacts on the sand probe. The electrical signal recorded gives an indication of the kinetic energy of the sand particles and beginning of sanding. However, signals from oil droplets, gas bubbles, and turbulent flow impacts may interfere with signal recordings from only produced sand particle impacts. These extra signals generated from other sources are termed background noise and need be filtered out before interpreting the recordings.

Research has shown that the intrusive ultrasonic probes are quite more efficient in gas flow as compared with liquid flow. Reasons being that, higher flow velocities are involved with gas and that will increase the kinetic energy of the solid particles to result in higher impacts and stronger signals being generated and detected. It is recommended that this detector be used at velocities higher than 3m/s.

4.5.3 Clamp-On Ultrasonic Detectors
This is a non-intrusive kind of sand detector and is the most common type of ultrasonic sand monitors. They record high frequency waves generated by particle impacts on the pipe wall. They are able to give an indication to the onset of sanding or gravel pack failure.

Background noise is equally experienced using this type of detector from gas bubbles, flow turbulence and droplets of liquid. Lower frequencies are generated from background noise as compared to higher frequencies from sand particle impacts. The process of filtering background noise from the normal sand

signals can be done based on the frequency band range, where signals with higher amplitudes than those from the background noise frequencies are recorded to obtain an appropriate sand impact rate (SIR).

These detectors are best located at about two-pipe diameter from a bend, where the most severe velocity direction of sand particles and stronger impacts will occur as seen in Figure 16.
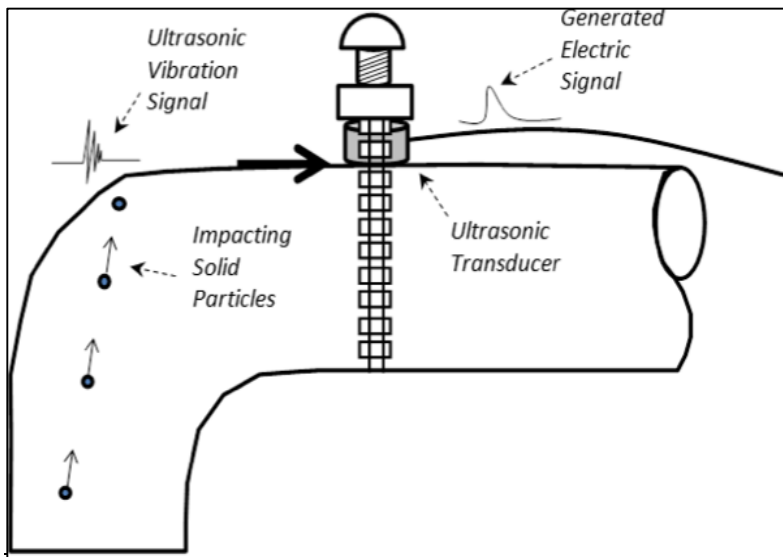

Figure 18: Schematic of clamp-on ultrasonic detector (Nabipour, et al. 2012)

4.5.4 Combining ER and Ultrasonic Monitoring Systems

In a bid to improve data quality and interpretation, efficiency and lower cost, the idea for integrating these sand monitoring techniques was conceived. The combination of these monitoring

systems make it possible to be able to give an early detection of sanding (from ultrasonic sensors) and also continue to provide information as regards sand velocity in the pipe (using ER probes). In other words, no data is lost from the onset of sanding to the flow of sand particles in pipes. More details about sand detectors and the integration of ER probes and ultrasonic detectors can be found in Nabipour, et al. (2012).

CHAPTER 5

SEPARATION OF SAND AND FINES FROM FLUIDS

Sand and fines production along with reservoir fluids has become a common trend in most oil and gas wells. Therefore, the need for surface separation of these unwanted solid particles becomes vital to prevent accumulation of these solid particles in production separators. These particles vary in concentration with a diameter often less than 250 microns. (Rawlins, et al. 2000).

Conventional methods of surface solid separation from reservoir fluids required periodical solid removal via sand jetting or shutting the system down and removing the sand by hand. Hydrocyclone was introduced as a more efficient and economic de-sanding alternative without system disruption. It requires less operator interaction and maintenance because they have no moving parts. (Rawlins, et al. 2000). The operation of hydro cyclone is discussed in the later part of this chapter.

5.1 Methodologies for Handling Sand and Fines

Two major methodologies for handling produced sand and fines will be discussed, based on a paper by Rawlins and Hewett, (2007). They are exclusion (subsurface) and inclusion (surface) methodologies.

5.1.1 Exclusion (Subsurface) Method

This method prevents sand particles from entering the wellbore using control techniques like mechanical retention (screen or slotted liner), chemical consolidation, gravel pack or a combination of these techniques. This sand handling method, which takes place downhole/subsurface, promotes the build-up of solids near the wellbore thereby increasing skin damage, which in turn adversely affects inflow production. On the other hand, the exclusion of sand downhole protects the production tubulars and surface equipment from erosion.

5.1.2 Inclusion (Surface) Method

This method allows sand into the wellbore and is produced along with reservoir fluids to separated and handled at the surface. The sand particles are being separated from the well fluids using a multiphase de-sander at the surface before or after the choke (pre or post). This method tends to reduce skin damage as solids are allowed to flow freely into the wellbore and this sustains or increases inflow production. However the free flow of solids into the wellbore could cause erosion of production tubulars and surface equipment, and might lead to production downtime if the solids eventually fill up the separators.

Rawlins and Hewett (2007) did a comparison of the performance and operability of both methods and concluded that the inclusion method is more cost effective than the exclusion method for mature fields, as it promotes a higher well productivity and becomes more cost advantageous as number of wells involved

increases. However, the cost for sand disposal also has to be taken into consideration.

5.2 Surface Sand Handling System

Rawlins, et al. (2000) listed five areas of solids handling in the oil and gas industry: separation, collection, cleaning, dewatering and haulage.

Separation

Separation is always the first step in handling produced sand and fines, and could be achieved through the use of de-sanders, sand jets or filters. A de-sander could each be placed on the water and oil outlets of a low-pressure separator to separate sand from both produced fluids. This is the system employed by Chevron for South Pass 78A platform in the Gulf of Mexico.

Collection

The sand after separation is normally collected in a central location, which could be a de-sander accumulator vessel or dedicated process sump tank. There the solids are collected and purged on an intermittent basis.

Cleaning

Cleaning is required is most cases to wash off adsorbed hydrocarbon or chemical contaminants from the surface of sand

particles. Though this process might not be necessary if the sand disposal method is onshore landfill.

Dewatering

Dewatering involves the use of gravity drain containers, such as hanging mesh bags or screen-lined bins for water removal. This process significantly reduces (by 90% in most cases) the volume of solid slurry to be disposed.

Haulage

The definition of haulage here is related to transport and disposal of sand. Sand and fines after separation can be disposed using several methods. In times past, it could be dumped overboard or simply used for road surfacing (Mathis 2003). From an environmental perspective, seafloor deposition is unacceptable owing to the chemical composition of the sand-liquid mixture. It is therefore required to ship the separated sand to a properly designed landfill or re-inject it directly at depth along with produced water or seawater to maintain pressure (Tronvoll , et al. 2001).

5.3 Hydrocyclones

Hydrocylones are considered as devices with no moving part due to the fact that the tangential inlet makes fluids rotate, instead of mechanically rotating the wall. (Holdich 2002). An illustration of a hydrocyclone and flow patterns is shown in Figure 19. Holdich

(2002) indicated three operational velocities present in a hydrocyclone: tangential, radial and axial velocity.
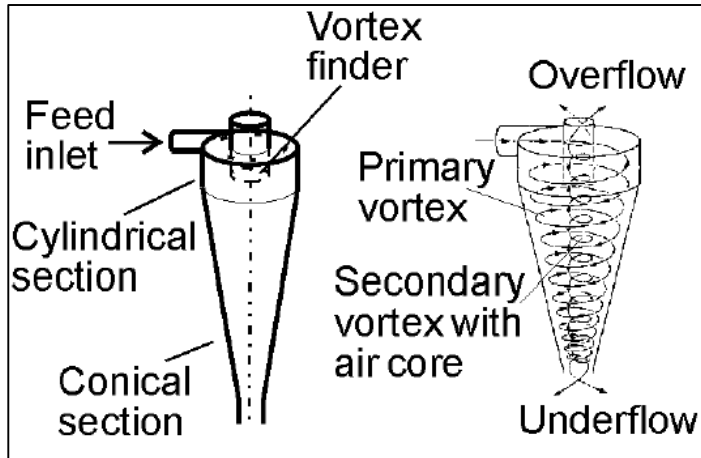
Figure 19: Schematic of hydrocyclone and flow patterns (Holdich 2002)

The tangential velocity, which could be up to 20 m/s for solids and liquid, is responsible for particles under the centrifugal field force. The radial velocity is significantly lower than the tangential, usually less than 0.1 m/s. It gives rise to the net flow of heavier phase (solids) outward towards the hydrocyclone wall and the net flow of lighter phase (liquid) towards the center. The axial velocity could be up to 3 m/s, and is responsible for splitting the phases between the two outlets by moving the heavier phase (solid) on the hydrocyclone wall axially towards the underflow and lighter phase (liquid) around the center, upward to the overflow.

The primary vortex (Figure 17) spirals down with solid particles to the underflow, while the secondary vortex spirals up with liquid to the overflow. In other words, the overflow is made up of lighter fluids and finer particles than the inlet feed, while the underflow contains denser and more concentrated suspension with coarser particle size distribution compared to the feed. (Holdich 2002).

5.3.1 Cut Size

Cut size (d_{50}) is defined as the particle size with 50% probability of capture by the hydrocyclone (Rawlins et al. 2000). When the forces pulling particles away from the center of the hydrocyclone (centrifugal force) is balanced by the liquid drag towards the center, the particles adopt an orbit at the Locus of Zero Vertical Velocity (LZVV). At the LZVV there is no net velocity in the axial direction. Particles here have equal chances (50% chance) of moving to either the overflow or underflow (Figure 18). Particles orbiting at radial distances less and greater than the LZVV will be in the secondary and primary vortex respectively. (Holdich 2002).
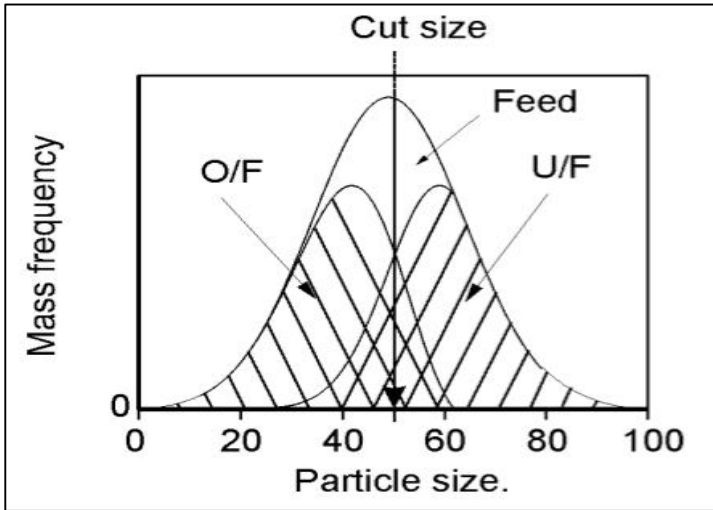
Figure 20: Idealized plot of size distributions indicating the cut size (Holdich 2002)

$$3\pi\mu dv_r = \pi d^3/_6 (\rho_P - \rho_L) r\omega^2$$

[5-1a]

Rearranging equation [5-1a] gives the cut size as:

$$d_{50} = \sqrt{18\mu v_r/_{(\rho_P - \rho_L) r\omega^2}}$$

[5-1b]

Where,

r = Radius of LZVV

v_r = Radial liquid velocity

ω = Angular velocity

CHAPTER 6
HYSYS PROCESS SIMULATOR

AspenTech's HYSYS software (version 7.3) was used in this work to obtain oil properties, such as viscosity and density, based on the volatile oil composition in Table A 6.

To start; a new case was opened and then fluid package added. Equation of State (EOS), Peng Robinson was used, as it is the preferred for oil and gas calculations. Then components were added, which were basically volatile oil components (Table A 6), in the same order. Water was added to the list of components to give a feel of a typical reservoir fluid composition of gas, oil and water.

Entering the simulation environment was the next step, where pipe segment was selected from the object palette. A mixer was used to give the multiphase flow condition of gas, oil and water. The necessary parameters (as shown in Table A 7) were specified. These values were assumed using typical values from previous literature works.

The mole fractions were equally specified with that of water as zero and one for reservoir oil/gas and water respectively (Figure B 2). The sum of mole fractions is often normalized if it is not equal to one. HYSYS calculated the output parameters: pressure, temperature, volumetric fractions, density, viscosity etc. (Figure B 3 and Figure B 5)

CHAPTER 7
DISCUSSION

Sand and fines production is one of the major issues plaguing oil and gas industries worldwide. As mentioned in chapter 2, majority of the world's hydrocarbon is obtained from North Sea, Gulf of Mexico, Middle East and Gulf of Guinea. These places all have one thing in common, that is sand production with a greater percent of the formations being unconsolidated. Sand management techniques have been put in place to address the issues of sanding.

A good sand production prediction method and early sand management implementation is advisable, most especially in unconsolidated formations where the tendency for sand and fines production is high, and would tend to always increase with oil and gas production time (Figure 2). In the Varg field, sand production was controlled at an early stage, which gave the advantage of reviewing several options and opting for the most economic means of sand control.

Sand production in some fields (Frog Lake and Lindbergh) was seen as a boost to oil production and this was attributed to either higher reservoir mobility or development of highly permeable zones due to sanding. On the other hand, this had to be checked by weighing the pros and cons of sanding and it led to the development of a model that links sand rate and reservoir

enhancement to forecast the economic outcome of sand production.

In other fields (Gullfaks, Zulia, Persia etc.), sand production is observed to hinder oil production and posed a major challenge. This could be as a result of reduced flow area for reservoir fluids due to partial blockage of flowlines by sand particles. After the installation of ESS in the Persian field, it was observed that oil production sprung up after a year (Figure 5).

In recent times, water production with oil is observed to be greater by a factor of three on the average i.e. for one barrel of oil produced, three barrels of water is produced. Studies have shown that more water production in a field indicates greater risk of sand production and this is related to the strength reducing effect water has on rocks as seen in Figure 7. (Wu and Tan 2005). Since water is normally injected during the later life of a well to boost depleted reservoir pressure (Figure 8), one can deduce that the greatest risk for sand production in a field is experienced during this period (water flooding stage).

Flow rates, fluid properties, pipe size, topography and pressure drop all play a role in determining the flow pattern of a multiphase fluid flow, which could be any of annular, slug, dispersed bubble, or stratified flow. The most challenging aspect of multiphase flow is that it could exist in many forms as two-phase flow (gas-liquid, liquid-liquid, solid-liquid, and solid-gas) and also as three-phase and quasi four-phase flow (Bratland 2010).

The determining factor for constant movement of sand and fines particles in tubing and pipelines is the fluid velocity. It has to be higher than the MTV to ensure particle movement. Fluid velocities lower than the MTV will most likely lead to sand bed formation on the base of pipelines, thus providing an enabling environment for corrosive agents to breed. On the other hand a high fluid velocity has greater tendencies of causing erosion on the walls of pipes. Hence, there has to be a check and balance of the fluid flow velocity to prevent sand bed formation and keep particle impact velocity at a minimum.

A velocity profile distribution for multiphase flow in horizontal pipe was computed and plotted for different flow regimes as shown in Figure B 6. Equation [4-14] was used to calculate the velocity of the sand particle at each particular point in the pipe cross-section. The average of the range of values for the constants A, B and C was obtained from Table A 4 and used in the equation. Fluid density, viscosity, volumetric liquid rate, gas and liquid hold-up were obtained from HYSYS simulation (Figure B 5). A particle diameter of 0.00025 m was used based on typical particle size found in unconsolidated reservoir in Niger Delta (Bello 2008).

It is observed that the annular and slug flow had the highest peak (i.e. at the pipe center) in the flow velocities of the sand particles of 13.2 m/s and 9.8 m/s respectively. This is logical and can be attributed to the fact that annular and slug flow contain considerable amount of gas (McLaury, et al. 2010), which is

normally located around the pipe center, with the liquid stream around the pipe wall.

A plot of gas and liquid hold up as a function of mixture velocity is shown in Figure B 7. Equation [4-15] was used to determine liquid hold-up for different ranges of mixture velocity assumed as shown in Appendix C2. It was observed that the liquid hold up dropped as the gas hold up increased with increasing mixture velocity.

Gas and liquid velocities were plotted against mixture velocity in Figure B 8, using Danielson (2007) drift model equation [4-6] to determine the gas velocity from mixture velocity, assuming empirical constant C to be 1.2. Liquid velocity was obtained using equation [4-10]. As expected the gas velocity showed a huge rise compared with liquid velocity. A plot of pressure drop versus superficial liquid and gas velocities was made, based on the Lockhart-Martinelli method for two-phase pressure drop calculations. The graph showed a positive slope for both fluids.

CHAPTER 8
CONCLUSION

Sand and fines production in the petroleum industry is a universal occurrence, thus making the study of multiphase gas-liquid-solid very necessary and vital to the growth of the industry. Three-phase flow patterns unlike two-phase and single phase is quite ambiguous and still requires further work to give simple expressions for gas-liquid-solid flow patterns in horizontal and vertical pipes.

The tendency for sand production to occur increases with water cut. Rocks and perforations tend to weaken in the presence of more water and this effect is more significant in rocks with high clay contents. It was deduced that sand production has a greater tendency to occur towards the late life of an oil and gas well, when reservoir pressure depletes or water breaks through.

Erosion of pipe walls is one of the major damages caused by sand and fines particles. Particle impact velocity is the most important parameter when dealing with sand erosion in pipes. Other important parameters are impact angle, sand sharpness and concentration, fluid velocity and properties. The detection of sand particles in pipes is usually centered around particle impacts on the pipe walls.

Produced sand and fines can either be eliminated at the subsurface using sand control methods or at the surface using a multiphase

desander. The combination of both methods will result in a more efficient sand handling process. However, economics will have to be considered, and in so doing surface management of produced sand has proven to be more cost effective than applying subsurface control methods in mature oil and gas fields.

Velocity of sand particles in pipe is to a large extent dependent of the fluid velocity, which would be higher with increase in the amount of gas present. Thus, sand and fines in annular and slug flow will tend to always have a higher particle flow velocity around the pipe cross-section center. Pressure drop along a pipe in a steady two-phase flow will normally tend to increase with increasing superficial velocities of the fluids.

REFERENCES

Abass, H H, H A Nasr-El-Din, and M H Ba Taweel. "Sand Control: Sand Characterization, Failure Mechanisms and Completion Methods." *SPE Annual Technical Conference and Exhibition.* San Antonio, Texas: SPE 77686, 2002.

Abubakar, M, I Lesor, S Aribo, and M B Umeleuma. "Comparative Study of Sand Control Methods in Niger Delta." *Journal of Petroleum Science Research*, October 2012: 57-64.

Adeyanju, O A, and L O Oyekunle. "Experimental Studies of Sand Production from Unconsolidated Sandstone Niger-Delta Petroleum Reservoir." *Nigeria Annual International Conference and Exhibition.* Abuja, Nigeria: SPE 151008, 2011.

—. "Hydrodynamics of Sand-Oil-Gas Multiphase Flow in a Near Vertical Well." *SPE Nigerian Annual International Conference and Exhibition .* Abuja, Nigeria: SPE 163036, 2012.

Andrews, J, H Kjørholt, and H Jøranson. "Production enhancement from sand management philosophy. A Case Study from Statfjord and Gullfaks." *SPE 6th European Formation Damage Conference.* Scheveningen, The Netherlands: SPE 94511, 2005.

Bagci, S, and A Al-Shareef. "Characterization of Slug Flow in Horizontal and Inclined Pipes." *SPE Production and Operations Symposium.* Oklahoma, USA: SPE 80930, 2003.

Bell, K J, and A C Mueller. "Pressure Drop." In *Wolverine Engineering Data Book 2*, 271-274. Wolverine Tube, Inc, 2001.

Bello, K O, M B Oyeneyin, and G F Oluyemi. "Minimum Transport Velocity Models for Suspended Particles in Multiphase Flow Revisited." *SPE ATCE.* Denver, Colorado: SPE 147045, 2011. 10.

Bello, O O. "Modelling Particle Transport in Gas-Oil-Sand Multiphase Flows and Its Applications to Production Operations." Dissertation, Faculty of Energy and Economic Sciences, Clausthal University of Technology, Ibadan,Nigeria, 2008.

Bratland, O. *Pipe Flow 2: Multiphase Flow Assurance.* 2010.

Byrne, M, A Slayter, and P McCurdy. "Improved Selection Criteria for Sand Control - When are "Fines" Fines?" *SPE International Symposium and Exhibition on Formation Damage Control.* Lafayette, Louisiana: SPE 128038, 2010.

Cathedral Energy. "Directional Drilling." 2013. http://www.cathedralenergyservices.com/services/drilling.php (accessed March 12, 2013).
Chen, J S, S Chen, M M Altunbay, and E Tyurin. "A New Method of Grain Size Determination for Sand Control Completion Applications." *SPE International Symposium and Exhibition.* Lafayette, Louisiana, USA: SPE 128011, 2010. 10.

Danielson , T J. "Sand Transport Modeling in Multiphase Pipelines." *Offshore Technology Conference.* Houston, Texas: OTC 18691, 2007.

Doan , Q, S M Ali, and A George. "Flow of Oil and Sand in a Horizontal Well." *5th Petroleum Conference.* South Saskatchewan, 1993.

Eriksen, J H, F Sanfilippo, A L Kvamsdal, and E Kleppa. "Orienting Live Well Perforating Technique Provides Innovative Sand-Control Method in the North Sea." *SPE Drilling and Completion* (SPE), 2001: 164-175.

Heavy Oil Science Center. "Types of Drilling." 2013. http://www.lloydminsterheavyoil.com/drillingtypes.htm (accessed March 15, 2013).

Helms, L. "Horizontal Drilling." 2013.
https://www.dmr.nd.gov/ndgs/newsletter/NL0308/pdfs/Ho
rizontal.pdf (accessed March 14, 2013).

Holdich, R G. *Fundamentals of Particle Technology.*
Loughborough: Midland Information Technology and
Publishing, 2002.

Hong'en, D, H Dandan, and C Wenxin. "Sand Production
Prediction and the Selection of Completion Methods for
Horizontal Wells in Intercampo Oil Field, Venezuela." *SPE Asia
Pacific Oil and Gas Conference and Exhibition.* Jakarta,
Indonesia: SPE 93821, 2005. 12.

King, R P. *Introduction to Practical Fluid Flow.* Oxford, 2002.

Ling, K, H Zhang, G Han, and Z Shen. "A New Approach to
Calculate Pressure Drop for Three-Phase Flow in Pipe." *SPE
International Production and Operations Conference and
Exhibition .* Doha, Qatar: SPE 151537, 2012.

Luo, W, S Xu, and F Torabi. "Laboratory Study of Sand
Production in Unconsolidated Reservoir." *SPE Annual
Technical Conference and Exhibition.* San Antonio, Texas: SPE
158619, 2012.

Maley, L C, and W P Jepson. "Liquid Holdup in Large-Diameter
Horizontal Multiphase Pipelines." *Journal of Energy Resources
Technology* 120 (September 1998): 185-192.

Maryam , D. "Oil Well Sand Production Control." *International
Applied Geological Congress.* Iran, 2010. 1996-2000.

Mathis, S P. "Sand Management: A Review of Approaches and
Concerns." *SPE European Formation Damage Conference.* The
Hague, The Netherlands: SPE 82240, 2003.

Mazurek, K A, R J Chalaturnyk, N Rajaratnam, and J D Scott.
"Transport of Fine Sand from a Wellborre." *Journal of
Canadian Petroleum Technology* 41, no. 4 (April 2002): 53-61.

McKay, I, P R Russ, and J W Mohr. "A Sand Management System for Mature Offshore Production Facilities." *International Petroleum Technology Conference.* Kuala Lumpur, Malaysia: IPTC 12784, 2008.

McLaury, B S, S A Shirazi, and E F Rybicki. "Sand Erosion in Multiphase Flow for Slug and Annular Flow Regimes." *NACE International Corrosion Conference and Expo .* Tulsa: NACE 10377, 2010.

McPhee, C A, Z R Lemanczyk, P Helderle, D Thatchaichawalit, and N Gongsakdi. "Sand Management in Bongkot Field, Gulf of Thailand: An Integrated Approach." *SPE Asia Pacific Oil and Gas Conference and Exhibition.* Brisbane, Australia: SPE 64467, 2000.

Michael, R. P. *Minimum Velocity Required to Transport Solid Particles from the 2H Evaporator to the Tank Farm.* U.S Department of Energy. 2012. http://sti.srs.gov/fulltext/tr2000263/tr2000263.html (accessed May 9, 2012).

Ming, J. P. and Jin, J. W. "Analysis of drag and lift coefficient expressions of bubbly flow system for low to medium Reynolds number ." *Nuclear Engineering and Design* (Elsevier), 2011: 2204–2213.

Muzychka, Y S, and M M Awad. "Asymptotic Generalizations of the Lockhart–Martinelli Method for Two Phase Flows." *Journal of Fluids Engineering*, March 2010.

Nabipour, A, B Evans, M Sarmadivaleh, and C Kalli. "Methods for Measurement of Solid Particles in Hydrocarbon Flow Streams." *SPE Asia Pacific Oil and Gas Conference and Exhibition.* Perth, Australia: SPE 158580, 2012.

Nigel, P B, and I H Nigel. *Slurry Handling - Design of Solid - Liquid Systems.* New York: Elsevier Science Publishers, 1991.

Odigie, M E, B S McLaury, S A Shirazi, and S Cremaschi. "Acoustic Monitor Threshold Limits for Sand Detection in Multiphase Flow Production System." *SPE International Conference and Exhibition .* Aberdeen: SPE 154378, 2012.

Pedersen , O A. *Properties of Oils and Natural Gases.* Gulf Publishing Company , 1989.

Pingshuang, W, Z Jianliang, and L Ming. "Sand Production Prediction of Weizhou12-1 Oilfield in Beibu Gulf in South China Sea." *SPE International Oil and Gas Conference and Exhibition.* Beijing: SPE 64623, 2000.

Rawlins, C H, and T J Hewett. "A Comparison of Methodologies for Handling Produced Sand and Solids to Achieve Sustainable Hydrocarbon Production." *European Formation Damage Conference .* Scheveningen, The Netherlands: SPE 107690, 2007.

Rawlins, C H, S E Staten, and I I Wang. "Design and Installation of a Sand Separation and Handling System for a Gulf of Mexico Oil Production Facility." *SPE Annual Technical Conference and Exhibition.* Dallas, Texas: SPE 63041, 2000.

Reza, S M, A S Gholam, and M B Abouzar. "Successful Applications of Expandable Sand Screen in Persian Oil Fields, Part 1." *SPE Production and Operations Conference and Exhibition.* Tunis, Tunisia: SPE 133364, 2010.

Schlumberger. *Schlumberger Oilfield Glossary.* 2013. http://www.glossary.oilfield.slb.com/search.cfm (accessed March 15, 2013).

Sereneworld. "Managing Sand Production: Risks and Rewards." 2013. http://www.senergyworld.com/SENERGYWORLD/media/Senergy/Training/public-courses/Managing%20sand%20production%20-%20risks%20and%20rewards_web.pdf (accessed March 28, 2013).

Sotgia , G. "Two-Phase Oil-Water, Three-Phase Oil-Water-Air Flows in Horizontal/Inclined Pipes; Pressure Drop and Flow Regime." Research, Department of Energetics, Polytechnic University of Milan, Milan, Italy, 2006.

Sunday, I, and F Andrew. "Sand Failure Mechanism and Sanding Parameters in Niger Delta Oil Reservoirs." *International Journal of Engineering Science and Technology* 2, no. 5 (2010): 777-782.

Tang, Y, M Wolff, P Condon, and K Ogden. "A Dynamic Wellbore Modeling for Sinusoidal Horizontal Well Performance with High Water Cut." *SPE Annual Technical Conference and Exhibition.* Anaheim, Canada: SPE 109262, 2007.

Thomas, J. D. "Sand Transport Modeling in Multiphase Pipelines." *Offshore Technology Conference.* Houston, Texas: OTC 18691, 2007. 11.

Thome, J R. *Engineering Databook 3.* Lausanne: Wolverine Tube, Inc, 2010.

Tronvoll , J, M B Dusseault, F Sanfilippo, and F J Santarelli. "The Tools of Sand Management." *SPE Annual Technical Conference and Exhibition.* New Orleans, Louisiana: SPE 71673, 2001.

Vincent, O N, S O Abiola, O O Felix, and J A Ajienka. "Sanding in Oil Well Reservoir Completions." *Nigeria Annual International Conference and Exhibition.* Abuja, Nigeria: SPE 163010, 2012. Weber, M. *Liquid - Solid Flow.* 2012. http://www.thermopedia.com/content/51/?tid=104&sn=1297 (accessed April 30, 2012).

Wu, B, and C P Tan. "Effect of Water-Cut on Sand Production – An Experimental Study." *Asia Pacific Oil & Gas Conference and Exhibition.* Jakarta, Indonesia: SPE 92715, 2005.

Yarlong, W., and C. C. Carl. "Enhanced Oil Production Owing to Sand Flow in Conventional and Heavy-Oil Reseroirs." *SPE Reservoir Evaluation & Engineering* (SPE), October 2001: 366-374.

APPENDIX A: Tables

Table A 1: Physical Properties of Sands and Fines (Rawlins and Hewett, 2007) and (Byrne, et al. 2010)

	Sand	*Fines*
Specific Gravity	2.5-2.9	2.6-2.8
Shape Factor	0.2-0.5	0.1-0.3
Size Range (μm)	50-1000	< 45
Conc. (ppmv)	5-100	< 1

Table A 2: Scale of Grade and Class Terms for Clastic Sediments (Byrne, et al. 2010)

φ Scale	Size Range	Wentworth Range	Name	Other Names
-8 to -∞	256- ∞ mm		Boulder	
-6 to -8	64-256 mm	2.5-10.1 in	Cobble	
-5 to -6	32-64 mm	1.26-2.5 in	Very coarse gravel	Pebble
-4 to -5	16-32 mm	0.63-1.26 in	Coarse gravel	Pebble
-3 to -4	8-16 mm	0.31-0.63 in	Medium gravel	Pebble
-2 to -3	4-8 mm	0.157-0.31 in	Fine gravel	Pebble
-1 to -2	2-4 mm	0.079-0.157 in	Very fine gravel	Pebble
0 to -1	1-2 mm	0.039-0.079 in	Very coarse sand	
1 to 0	0.5-1 mm	0.020-0.039 in	Coarse sand	
2 to 1	0.25-0.5mm	0.010-0.020 in	Medium sand	
3 to 2	125-250 μm	0.0049-0.010 in	Fine sand	
4 to 3	62.5-125 μm	0.0025-0.0049 in	Very fine sand	
8 to 4	3.9-62.5 μm	0.00015-0.0025 in	Silt	Mud
∞ to 8	1/∞-3.9 μm		Clay	Mud
∞ to 10	1/∞-1 μm		Colloid	Mud

Table A 3: Drag Relationship for Spheres (Nigel and Nigel 1991)

Flow regime and range of Reynolds Number (Re_p)	Relation for drag coefficient (C_d)
Stokes Law $Re_p \leq 1$	$C_d = 24Re_p^{-1}$
Intermediate $1 < Re_p \leq 1000$	$C_d = 24Re_p^{-1}\left(1 + 0.15Re_p^{0.687}\right)$
Newton's Law $1000 < Re_p \leq 2 \times 10^5$	$C_d = 0.44$

Table A 4: Constants for Velocity Equation [4-14] (Bello, et al. 2011)

Flow Pattern	A	B	C
Disp. Bubble	3-4	0.2-0.5	0.1-0.5
Annular Flow	1-2	0.2-1	0.1-0.5
Slug Flow	2.5-3.5	0.3-0.5	1-1.5

Table A 5: Constants for MTV Equation [4-5]

MTV	A	B
Vertical Pipe	4-6	0.1-1

Table A 6: Volatile Oil Composition (Pedersen 1989)

Component	Mol%
N_2	1.67
CO_2	2.18
C_1	60.51
C_2	7.52
C_3	4.74
C_4 (i+n)	4.12
C_5 (i+n)	2.97
C_6 (i+n)	1.99
C_7	2.45
C_8	2.41
C_9	1.69
C_{10}	1.42
C_{11}	1.02
C_{12+}	5.31

Table A 7: HYSYS Input Parameters

Name	Tubing	Pipeline
Length, m	4000	5.50E+04
Elevation Change, m	4000	0
Outer Diameter, mm	770	900
Inner Diameter, mm	640	770
Increments	15	550
Ambient Temp. ºC	20	5
Overall HTC W/m^2-C	5	5
Temperature, ºC	90	-
Pressure, bar	300	-
Molar Flow, MMSCFD	1000	-

APPENDIX B: Figures
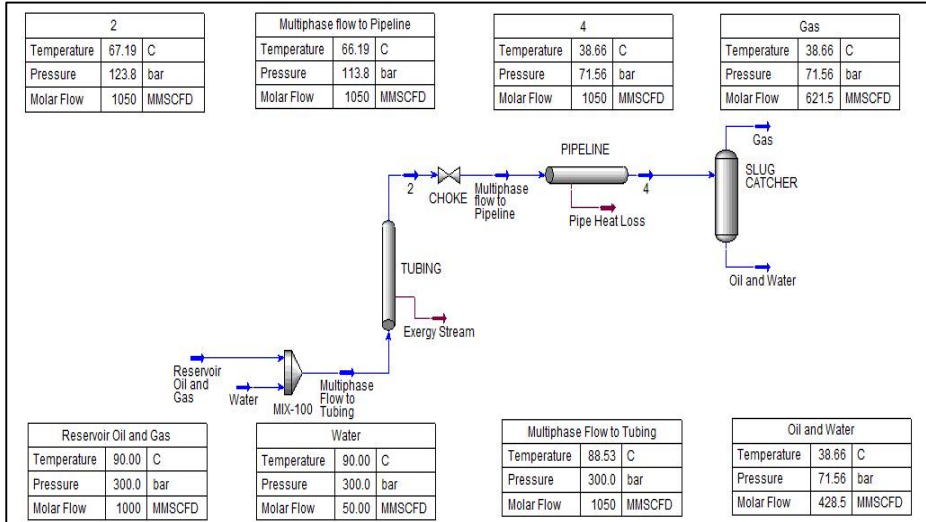
Figure B 1: HYSYS Simulation Environment

	Mole Fractions	Vapour Phase	Aqueous Phase
Nitrogen	0.015905	0.016615	0.000060
CO2	0.020762	0.021668	0.000540
Methane	0.576286	0.602101	0.000017
Ethane	0.071619	0.074827	0.000000
Propane	0.045143	0.047165	0.000000
n-Butane	0.039238	0.040996	0.000000
n-Pentane	0.028286	0.029553	0.000000
n-Hexane	0.018952	0.019801	0.000000
n-Heptane	0.023333	0.024379	0.000000
n-Octane	0.022952	0.023981	0.000000
n-Nonane	0.016095	0.016816	0.000000
n-Decane	0.013524	0.014130	0.000000
n-C11	0.009714	0.010149	0.000000
n-C12	0.050571	0.052837	0.000000
H2O	0.047619	0.004983	0.999382

Figure B 2: Composition of multiphase flow to tubing

Stream Name	Multiphase Flow	Vapour Phase	Aqueous Phase
Vapour / Phase Fraction	0.95712	0.95712	0.04288
Temperature [C]	88.531	88.531	88.531
Pressure [bar]	300.00	300.00	300.00
Actual Vol. Flow [m3/h]	4714.8	4673.1	41.704
Mass Enthalpy [kJ/kg]	-3110.1	-2869.2	-15531
Mass Entropy [kJ/kg-C]	3.7728	3.7725	3.7881
Molecular Weight	40.643	41.656	18.030
Molar Density [kgmole/m3]	11.092	10.711	53.767
Mass Density [kg/m3]	450.82	446.19	969.40
Std. Liquid Mass Density [kg/	443.57	438.78	1015.0
Molar Heat Capacity [kJ/kgm	112.55	114.11	77.721
Mass Heat Capacity [kJ/kg-C	2.7692	2.7393	4.3107
Thermal Conductivity [W/m-K	<empty>	9.0553e-002	0.67509
Viscosity [cP]	<empty>	7.7872e-002	0.31664
Surface Tension [dyne/cm]	<empty>	<empty>	60.723
Specific Heat [kJ/kgmole-C]	112.55	114.11	77.721
Z Factor	<empty>	0.93137	0.18555
Vap. Frac. (molar basis)	0.95712	0.95712	4.2876e-002
Vap. Frac. (mass basis)	0.98098	0.98098	1.9020e-002
Vap. Frac. (Volume Basis)	0.99021	0.99021	9.7929e-003
Molar Volume [m3/kgmole]	9.0153e-002	9.3359e-002	1.8599e-002

Figure B 3: Properties of multiphase flow to tubing

	Mole Fractions	Vapour Phase	Liquid Phase	Aqueous Phase
Nitrogen	0.015905	0.024682	0.005524	0.000024
CO2	0.020762	0.024938	0.017248	0.000427
Methane	0.576286	0.798718	0.332592	0.000003
Ethane	0.071619	0.075184	0.074669	0.000000
Propane	0.045143	0.034524	0.064878	0.000000
n-Butane	0.039238	0.019842	0.070467	0.000000
n-Pentane	0.028286	0.008996	0.058146	0.000000
n-Hexane	0.018952	0.003665	0.042231	0.000000
n-Heptane	0.023333	0.002725	0.054466	0.000000
n-Octane	0.022952	0.001601	0.055073	0.000000
n-Nonane	0.016095	0.000677	0.039236	0.000000
n-Decane	0.013524	0.000348	0.033273	0.000000
n-C11	0.009714	0.000150	0.024039	0.000000
n-C12	0.050571	0.000505	0.125526	0.000000
H20	0.047619	0.003445	0.002634	0.999545

Figure B 4: Composition of multiphase flow to pipeline

Stream Name	Multiphase flow	Vapour Phase	Liquid Phase	Aqueous Phase
Vapour / Phase Fraction	0.55468	0.55468	0.40064	0.04467
Temperature [C]	66.189	66.189	66.189	66.189
Pressure [bar]	113.76	113.76	113.76	113.76
Actual Vol. Flow [m3/h]	8443.2	5833.5	2566.7	42.988
Mass Enthalpy [kJ/kg]	-3154.1	-4081.2	-2405.3	-15647
Mass Entropy [kJ/kg-C]	3.7918	7.0368	2.4340	3.5303
Molecular Weight	40.643	21.268	69.989	18.026
Molar Density [kgmole/m3]	6.1941	4.9727	8.1633	54.348
Mass Density [kg/m3]	251.74	105.76	571.34	979.70
Std. Liquid Mass Density [kg/	<empty>	<empty>	629.40	1015.0
Molar Heat Capacity [kJ/kgm	106.26	60.249	173.13	77.799
Mass Heat Capacity [kJ/kg-C	2.6144	2.8328	2.4737	4.3158
Thermal Conductivity [W/m-K	<empty>	4.7571e-002	8.7833e-002	0.65913
Viscosity [cP]	<empty>	1.7089e-002	0.20437	0.42252
Surface Tension [dyne/cm]	<empty>	<empty>	8.3854	64.819
Specific Heat [kJ/kgmole-C]	106.26	60.249	173.13	77.799
Z Factor	<empty>	0.81083	0.49393	7.4190e-002
Vap. Frac. (molar basis)	0.55468	0.55468	0.40064	4.4673e-002
Vap. Frac. (mass basis)	0.29026	0.29026	0.68993	1.9814e-002
Vap. Frac. (Volume Basis)	0.41280	0.41280	0.57700	1.0201e-002
Molar Volume [m3/kgmole]	0.16145	0.20110	0.12250	1.8400e-002

Figure B 5: Properties of multiphase flow to pipeline
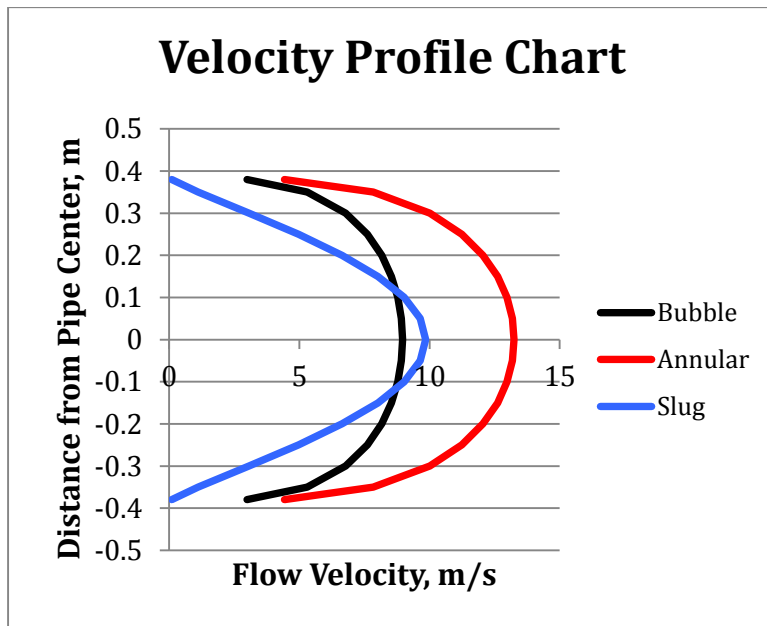
Figure B 6: Velocity profile distribution in multiphase horizontal pipe flow

93
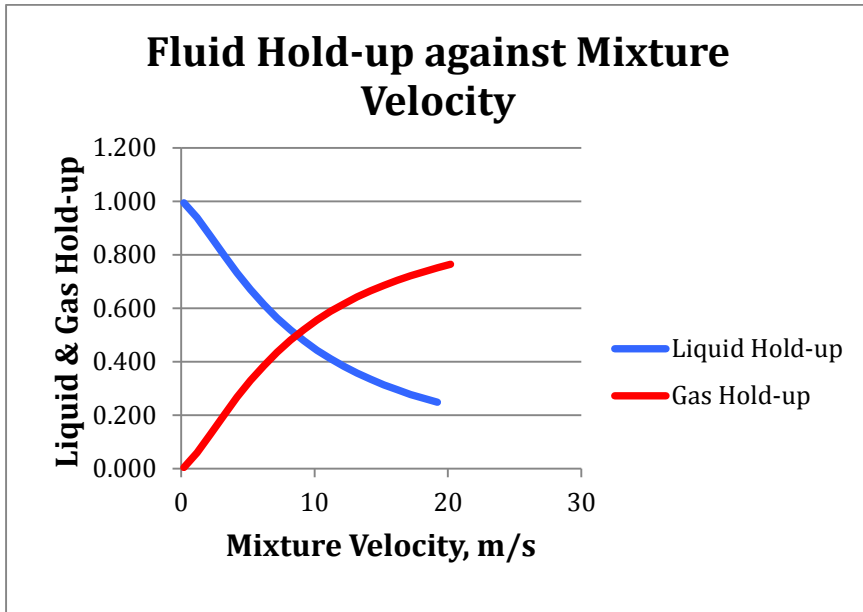
Figure B 7:Plot of liquid and gas hold-up versus mixture velocity
for Slug Flow
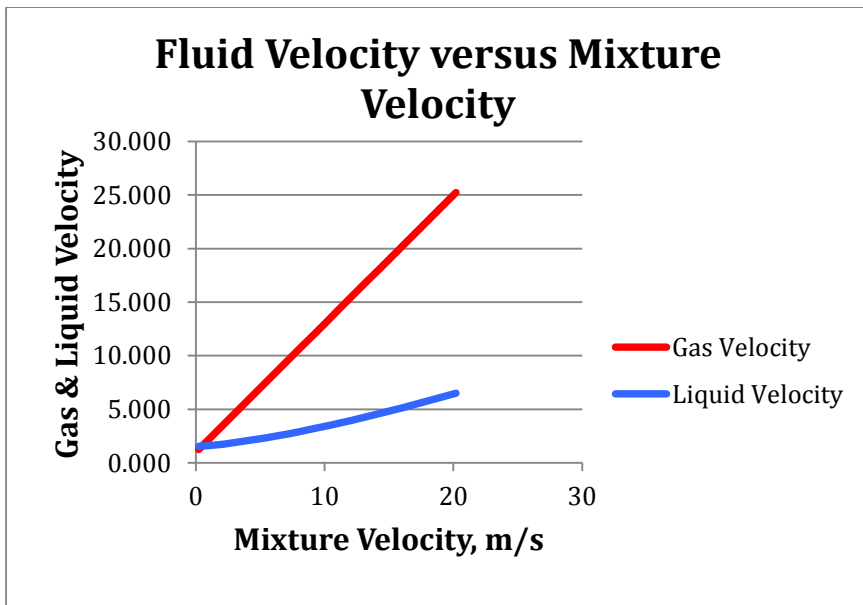
Figure B 8: Plot of gas and liquid velocity versus mixture velocity
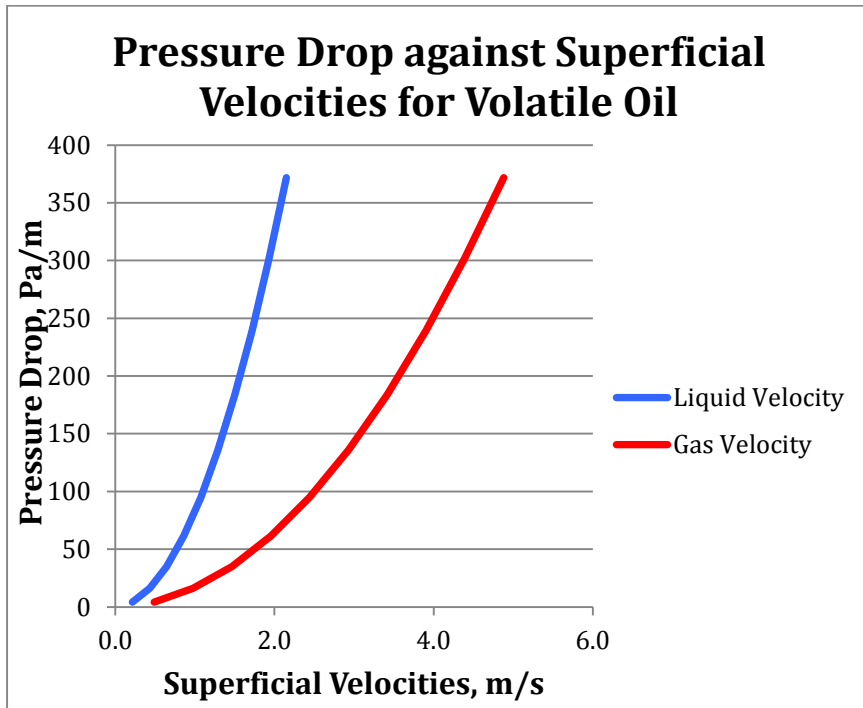
Figure B 9: Pressure drop versus superficial liquid and gas
velocities for volatile oil

APPENDIX C: Excel Calculations

C1: Computation of Velocity Profile

Parameters	Values	Units	Parameters	Values	Units
Particle Diameter, d_P	0.00025	m	Liquid Hold-up, H_L	0.400	-
Fluid Viscosity, μ	0.000215	$Pa.s$	Fluid Mixture Density, ρ_M	330.8	Kg/m^3
Particle Density, ρ_P	2650	Kg/m^3	Sand Velocity, v_S	0.135	m/s
Gas Density, ρ_G	105.0	Kg/m^3	Reynolds Number, Re	77.88	-
Liquid Density, ρ_L	571.0	Kg/m^3	Friction factor, f	0.822	-
Aqueous Density	979.7	Kg/m^3	Pipe Radius, R	0.385	m
Gas Hold-up, H_G	0.555	-	g	9.81	m/s^2

Flow Pattern	r	Velocity Profle, V_R		
	m	m/s	m/s	m/s
		Bubble	Annular	Slug
	-0.38	2.993	4.423	0.102
	-0.35	5.302	7.835	1.103
	-0.3	6.774	10.01	3.061
	-0.25	7.61	11.24	4.965
	-0.2	8.16	12.06	6.644
	-0.15	8.53	12.61	8.01
	-0.1	8.78	12.97	9.02
	-0.05	8.92	13.18	9.64
	0	8.97	13.25	9.84
	0.05	8.92	13.18	9.64
	0.1	8.78	12.97	9.02
	0.15	8.53	12.61	8.01
	0.2	8.16	12.06	6.644
	0.25	7.61	11.24	4.965
	0.3	6.774	10.01	3.061
	0.35	5.302	7.835	1.103
	0.38	2.993	4.423	0.102

C2: Calculation of Fluid Velocity and Hold-up

Parameters	Values	Units	Parameters	Values	Units
Gas Density, ρ_G	105.0	Kg/m^3	Pipeline Cross-sectional Area, A	0.465	m^2
Liquid Density, ρ_L	571.0	Kg/m^3	g	9.81	m/s^2
Bubble Rise Velocity, v_o	0.993	m/s	C	1.2	-
Volumetric Liquid Rate, Q_L	0.713	m^3/s	D	0.77	m

Mixture Velocity	Liquid Hold-up	Gas Velocity	Liquid Velocity	Gas hold-up
(m/s)	$(-)$	(m/s)	(m/s)	(m/s)
0.2	0.995	1.233	1.540	0.005
1.2	0.940	2.433	1.630	0.060
2.2	0.870	3.633	1.760	0.130
3.2	0.800	4.833	1.916	0.200
4.2	0.732	6.033	2.092	0.268
5.2	0.670	7.233	2.286	0.330
6.2	0.614	8.433	2.495	0.386
7.2	0.564	9.633	2.717	0.436
8.2	0.519	10.83	2.952	0.481
9.2	0.479	12.03	3.198	0.521
10.2	0.443	13.23	3.455	0.557
11.2	0.412	14.43	3.723	0.588
12.2	0.383	15.63	3.999	0.617
13.2	0.358	16.83	4.285	0.642
14.2	0.335	18.03	4.579	0.665
15.2	0.314	19.23	4.881	0.686
16.2	0.295	20.43	5.191	0.705
17.2	0.278	21.63	5.509	0.722
19.2	0.248	24.03	6.166	0.752
20.2	0.236	25.23	6.504	0.764

C3: Lockhart-Martinelli Method for Two-Phase Pressure Drop

Pipe Roughness	0.000045	m		
Pipe Diameter	0.77	m		
Cross-sectional Area	0.466	m^2		
Liquid Density	571	kg/m^3		
Gas Density	105	kg/m^3		
Liquid Viscosity	0.204	cp	0.000204	$Pa.s$
Gas Viscosity	0.011	cp	0.000011	$Pa.s$
Volumetric Liquid Rate	2567	m^3/h	0.713	m^3/s
Volumetric Gas Rate	5833.5	m^3/h	1.620	m^3/s

	Liquid	Gas	Units
Mass Flow Rate	407.1	170.1	kg/s
Mass Flux	874.3	365.3	kg/m^2s
Reynolds Number	330000.7	25570017.3	
Friction Factor (Haaland Equation)	0.015	0.011	−
Pressure Gradient	12.72	9.049	Pa/m
Lockhart-Martinelli Factor	1.186	1.186	−
Pressure Drop Multiplier	4.110	4.874	−
Total Pressure gradient	214.9	214.9	Pa/m